Check for updates

J Physiol 604.3 (2026) pp 1463–1484

The Journal of Physiology

Effect of varying driving pressure and respiratory rate on ventilator-induced lung injury in healthy and injured lungs: An experimental animal study

Davide Raimondi Cominesi[1], Vanessa Zambelli[1], Emma J. Murphy[2,3], Roberta Garberi[1], Aurora Magliocca[4], Roberto Fumagalli[1,5], Giacomo Bellani[6,7], Giuseppe Foti[1,8], Maurizio Cereda[9], John G. Laffey[10,11] and Emanuele Rezoagli[1,8]

[1]*School of Medicine and Surgery, University of Milano-Bicocca, Monza, Italy*
[2]*Bioengineering Organ-on-Chip Research Group, Centre for Applied Bioscience Research, Technological University of the Shannon–Midwest Campus, Limerick, Ireland*
[3]*RISM Institute, Technological University of the Shannon–Midlands Campus, Athlone, Westmeath, Ireland*
[4]*Department of Pathophysiology and Transplantation, University of Milan, Milan, Italy*
[5]*Department of Emergency Medicine, ASST Grande Ospedale Metropolitano Niguarda, Milan, Italy*
[6]*Centre for Medical Sciences–CISMed, University of Trento, Trento, Italy*
[7]*Department of Anesthesia and Intensive Care, Santa Chiara Hospital, APSS Trento, Largo, Trento, Italy*
[8]*Department of Emergency and Intensive Care, Fondazione IRCCS San Gerardo dei Tintori, Monza, Italy*
[9]*Department of Anesthesia, Critical Care and Pain Medicine, Harvard Medical School, Boston, MA, USA*
[10]*Anaesthesia and Intensive Care Medicine, School of Medicine, Clinical Sciences Institute, Galway University Hospitals, Galway, Ireland*
[11]*School of Medicine, Regenerative Medicine Institute (REMEDI) at CÚRAM Centre for Research in Medical Devices, National University of Ireland Galway, Galway, Ireland*

Handling Editors: Vaughan Macefield & Frank Powell

The peer review history is available in the Supporting Information section of this article (https://doi.org/10.1113/JP289904#support-information-section).

Davide Raimondi Cominesi, M.D., is a resident in Anesthesia and Intensive Care and a Ph.D. candidate in Translational and Molecular Medicine at the University of Milano-Bicocca. After earning his medical degree from the University of Milan, he joined the University of Milano-Bicocca in Monza, Italy, for his residency and doctoral training, focusing on respiratory physiology and mechanical ventilation in the Laboratory of Respiratory Pathophysiology led by Prof. Emanuele Rezoagli. He is currently pursuing a postdoctoral fellowship in the Department of Critical Care Medicine at St Michael's Hospital, Toronto, in the experimental laboratory directed by Prof. Laurent Brochard. **Vanessa Zambelli**, Ph.D., is a senior postdoctoral researcher at the University of Milano-Bicocca, Monza, Italy, working in the Laboratory of Respiratory Pathophysiology led by Prof. Emanuele Rezoagli. After graduating in Pharmaceutical Biotechnology, she obtained her Ph.D. in Biomedical Technologies from the University of Milano-Bicocca, focusing on advanced lung imaging techniques to study acute respiratory failure. She has extensive experience in preclinical experimental research, particularly in respiratory pathophysiology and lung imaging in rodent models of respiratory failure under mechanical ventilation. Since 2007, her research has focused on innovative therapeutic and ventilatory strategies for acute and chronic lung injury, with a strong emphasis on diagnostic advances through the application of micro-computed tomography.

D. R. Cominesi and V. Zambelli are co-first authors.

© 2025 The Author(s). *The Journal of Physiology* published by John Wiley & Sons Ltd on behalf of The Physiological Society.

DOI: 10.1113/JP289904

This is an open access article under the terms of the Creative Commons Attribution License, which permits use, distribution and reproduction in any medium, provided the original work is properly cited.

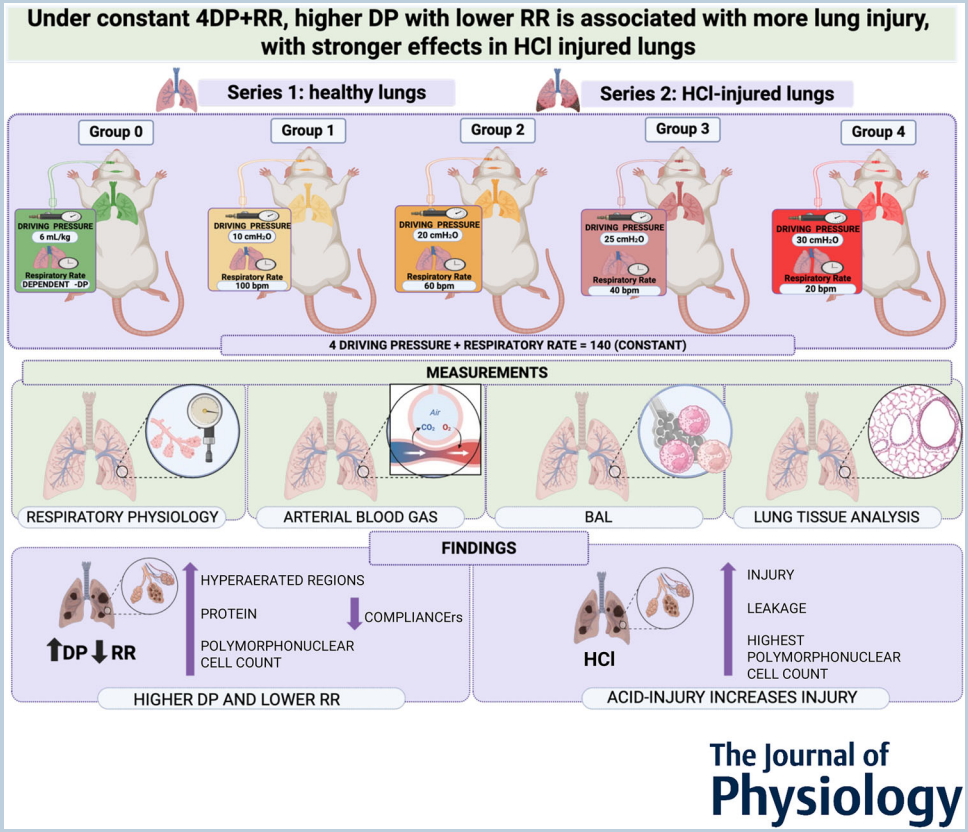

Abstract figure legend Top: experimental groups for the two series of rats: five combinations of driving pressure (DP) and respiratory rate (RR), maintaining a constant 4DP+RR value of 140, were applied for 4 h in healthy lungs (Series 1) and 2 h in HCl-injured lungs (Series 2). Middle: measurements included gas exchange, respiratory mechanics, lung microCT, bronchoalveolar lavage (BAL) analysis and histology to evaluate inflammation and structural damage. Bottom: despite a constant 4DP+RR, higher DP with lower RR resulted in reduced respiratory system (rs) compliance, increased protein leakage and greater polymorphonuclear cell infiltration, indicating regionally heterogeneous mechanical stress and injury progression. These effects were more pronounced in HCl-injured lungs.

Abstract Ventilator-induced lung injury (VILI) is a major complication of mechanical ventilation. A combined index of driving pressure (DP) and respiratory rate (RR), expressed as 4DP+RR, has been proposed to predict VILI risk. We investigated whether different combinations of DP and RR, whilst keeping 4DP+RR constant, result in different degrees of VILI in healthy (Series 1) and hydrochloric acid-injured rat lungs (Series 2). Rats were ventilated for 4 h (Series 1) or 2 h (Series 2) using five combinations of DP and RR, targeting a constant 4DP+RR equal to 140. We assessed gas exchange, partitioned respiratory mechanics, lung micro-computed tomography (microCT), bronchoalveolar lavage (BAL) and alveolar tissue histology. In Series 1, the highest DP with the lowest RR, led to impaired gas exchange, compliance reduction and increased inflammation, with evidence of a threshold effect in clinical parameters and a progressive increase in histological damage. In Series 2, the lung damage progressed linearly with increasing DP and decreasing RR. Despite a constant 4DP+RR, mechanical power (MP) paradoxically decreased as DP increased. In Series 1, inflammation occurred before detectable tissue damage. A threshold effect in clinical markers (oxygenation, compliance and microCT) alongside progressively increasing histological injury suggests that early lung injury may follow a two-phase progression. In Series 2, VILI progressed linearly with increasing DP and decreasing RR despite a constant 4DP+RR load. These findings support a complex interplay between DP, RR and the spatial distribution of energy dissipation as key determinants of VILI.

© 2025 The Author(s). *The Journal of Physiology* published by John Wiley & Sons Ltd on behalf of The Physiological Society.

14697793, 2026, 3, Downloaded from https://physoc.onlinelibrary.wiley.com/doi/10.1113/JP289904 by Universita Milano Bicocca, Wiley Online Library on [16/03/2026]. See the Terms and Conditions (https://onlinelibrary.wiley.com/terms-and-conditions) on Wiley Online Library for rules of use; OA articles are governed by the applicable Creative Commons License

(Received 8 August 2025; accepted after revision 12 November 2025; first published online 16 December 2025)
Corresponding author E. Rezoagli: School of Medicine and Surgery, University of Milano-Bicocca, Via Cadore 48, 20900, Monza, Italy. Email: emanuele.rezoagli@unimib.it

Key points

- Ventilator-induced lung injury (VILI) is a major complication of mechanical ventilation; the index combining driving pressure (DP) and respiratory rate (RR) - 4DP+RR - has been proposed to estimate the risk of VILI.
- Different combinations of DP and RR, while keeping 4DP+RR constant, may exert distinct effects on lung injury.
- We show that higher DP with lower RR exacerbates lung injury, despite a fixed 4DP+RR, and pre-injured lungs exhibit heightened vulnerability as compared to healthy lungs.
- Transpulmonary DP correlates strongly with structural injury as assessed by lung micro-Computed Tomography and histology, whereas mechanical power shows an unexpected inverse trend as DP increases and RR decreases.
- These findings demonstrate that a fixed 4DP+RR does not ensure lung protection and highlight DPRR interactions and spatial energy dissipation as key determinants of VILI progression.

Introduction

Mechanical ventilation plays an important role in the management of critically ill patients, but it can contribute to lung injury. This supports the need for protective ventilation strategies (Rezoagli et al., 2022; Slutsky & Ranieri, 2013). However, a critical clinical challenge remains. It is currently not possible to determine with certainty whether a specific set of ventilator settings is causing harm in each individual, in terms of both lung function and structure, as well as inflammation and alveolar capillary leakage.

Injured lungs are susceptible to ventilator induced lung injury (VILI) through various mechanisms, including alveolar overdistention (volutrauma), barotrauma, atelectotrauma and inflammation, especially in the absence of lung-protective strategies (Dreyfuss & Hubmayr, 2016; Gajic et al., 2005; Lee & Slutsky, 2001; Tremblay & Slutsky, 1998).

Amongst the mechanical factors contributing to VILI, driving pressure (DP) has been strongly associated with increased lung inflammation in acute respiratory distress syndrome (ARDS) patients, reinforcing the importance of limiting overdistension to mitigate lung injury (Bellani et al., 2011). Other respiratory variables, including respiratory rate (RR) (Rich et al., 2003) and inspiratory airflow (Fujita et al., 2007), have also been implicated in VILI development. These findings suggest that lung injury depends on a combination of mechanical forces exerted on lung tissues during ventilation.

Given the complexity of VILI pathophysiology, mathematical models based on primary ventilator parameters were reported as promising tools to predict patient outcomes in ARDS. Amongst these, mechanical power (MP) – a composite index quantifying the total energy delivered to the lungs per unit time – has been proposed as a key determinant of VILI development (Gattinoni et al., 2016; Tonetti et al., 2017). Experimental studies have demonstrated that VILI develops when an MP threshold is exceeded (Cressoni et al., 2016; Romitti et al., 2022).

More recently, a simplified model combining DP and RR as 4DP+RR has been introduced, reflecting the relative contribution of these two parameters to lung injury, with DP having approximately four times the weight of RR. This approach is based on the observation that both variables are key components of MP and contribute synergistically to VILI. Costa et al. (2021) demonstrated that this simplified index offers a practical alternative to full MP calculations. The 4DP+RR model showed similar predictive performance for mortality compared to MP in a large cohort of ARDS patients, supporting its potential as a clinically useful tool for ventilator management.

The quantification of the 4DP+RR index has never been explored in both healthy and injured models. We hypothesise that, at a constant value of 4DP+RR, the degree of VILI varies depending on the specific combination of DP and RR used, and that this variability is more pronounced in the presence of pre-existing lung injury. This is based on prior evidence that DP is a key determinant of lung damage, and that injured lungs are more sensitive to mechanical strain due to reduced

© 2025 The Author(s). *The Journal of Physiology* published by John Wiley & Sons Ltd on behalf of The Physiological Society.

14697793, 2026, 3, Downloaded from https://physoc.onlinelibrary.wiley.com/doi/10.1113/JP289904 by Universita Milano Bicocca, Wiley Online Library on [16/03/2026]. See the Terms and Conditions (https://onlinelibrary.wiley.com/terms-and-conditions) on Wiley Online Library for rules of use; OA articles are governed by the applicable Creative Commons License

compliance and altered structure (Cereda et al., 2016; Tonetti et al., 2017).

In this experimental preclinical study in healthy and lung-injured rats, we aim to assess the correlation between different combinations of DP and RR within the same 4DP+RR and VILI development, and to determine whether primary lung injury modifies this relationship.

Further, we aim to explore, within each group, whether changes in hypoaerated lung volume – assessed by micro-computed tomography (microCT) – are associated with respiratory variables of stress (i.e., transpulmonary driving pressure and MP).

Methods

Ethical approval

The study was reviewed and approved by the Italian Ministry of Health (486/2022 PR; FB7CC.57) and by the Animal Care Unit of the University of Milano-Bicocca, Monza, Italy.

Animals

Male Sprague–Dawley rats weighing between 260 and 370 g (Envigo RMS S.r.l., Udine, Italy) were used for these experiments (Tables 1 and 2). Animals were housed two per cage in a limited-access animal facility, with room temperature at 20 ± 2°C and relative humidity set at 55 ± 10%. Artificial lighting provided a 12 h light/12 h dark (07.00–19.00 h) cycle. Food and water were available *ad libitum* (24/7). Before the experiment, the general conditions of the animals were assessed daily. The care and husbandry of animals were in conformity with the institutional guidelines, following Italian and European laws and policies. In full respect of the reduction principle of the 3Rs (Díaz et al., 2020), the number of animals/groups was selected to obtain reliable results and enough biological samples to perform the analysis planned.

All experimental procedures were conducted in accordance with *The Journal*'s policies and ethical standards for animal research.

Experimental protocol

The experimental design (Fig. 1) included two series of rats, each divided into five experimental groups:

Series 1: healthy rats anaesthetised and mechanically ventilated for 4 h.

Series 2: hydrochloric acid (HCl)-induced lung-injured rats anaesthetised and mechanically ventilated for 2 h.

Rats were anaesthetised with intraperitoneal ketamine (100 mg/kg) and xylazine (4 mg/kg), orotracheally intubated and connected to a ventilator (Inspira ventilator, Harvard Apparatus, Holliston, MA, USA) in

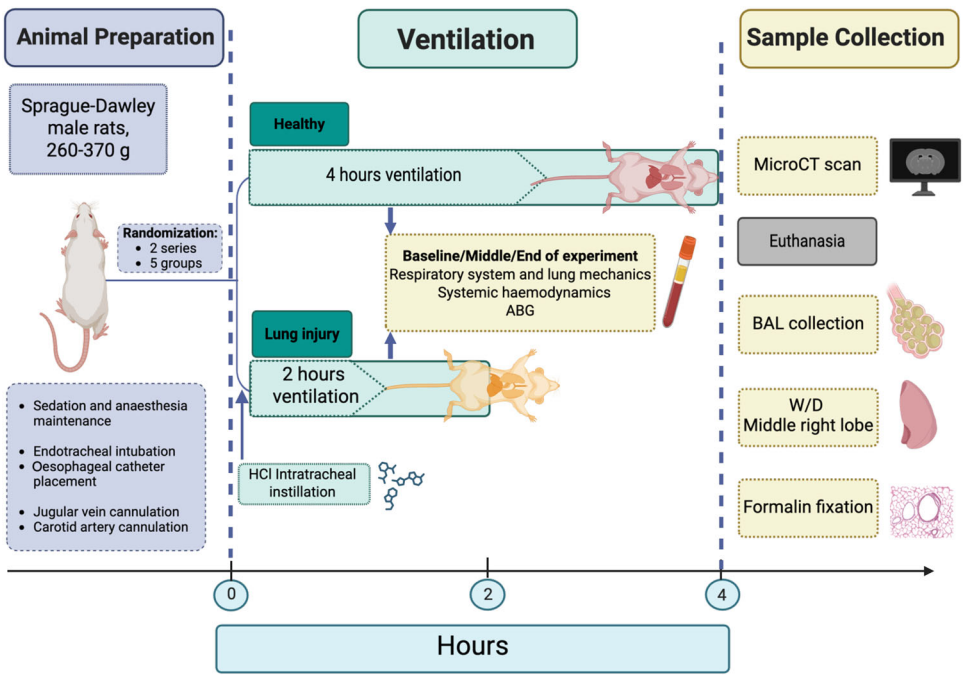

Figure 1.
Experimental protocol showing animal preparation, ventilation duration, and timing of physiological assessments and sample collection. ABG, arterial blood gas; BAL, broncho-alveolar lavage; microCT, micro-computed tomography scan; W/D, wet to dry ratio.

© 2025 The Author(s). *The Journal of Physiology* published by John Wiley & Sons Ltd on behalf of The Physiological Society.

14697793, 2026, 3, Downloaded from https://physoc.onlinelibrary.wiley.com/doi/10.1113/JP289904 by Universita Milano Bicocca, Wiley Online Library on [16/03/2026]. See the Terms and Conditions (https://onlinelibrary.wiley.com/terms-and-conditions) on Wiley Online Library for rules of use; OA articles are governed by the applicable Creative Commons License

Table 1. Series 1: Healthy rats undergoing mechanical ventilation for 4 h. Variables assessed in the study are categorised by groups and evaluated at two different time points (start and end). BAL polymorphonuclear cells are expressed as a percentage relative to a total of 200 cells evaluated under the microscope. Data are presented as mean ± SD and *P*-values correspond to ordinary one-way ANOVA or Kruskal–Wallis test for variables measured across groups, and to the time × group interaction from a mixed-effects model for variables measured across groups over time (start and end of the experiment). Thirty-six animals were included in this experimental series. The mean weight across all animals was 320 ± 19 g, with no significant differences in weight observed between the groups (*P* = 0.9735).

Series 1	Group 0 (DP at 6 mL/kg V_T, RR to reach 140; *n* = 5)	Group 1 (DP 10, RR 100; *n* = 8)	Group 2 (DP 20, RR 60; *n* = 7)	Group 3 (DP 25, RR 40; *n* = 8)	Group 4 (DP 30, RR 20; *n* = 8)	*P*
Body weight (g)	325 ± 13	321 ± 20	316 ± 17	321 ± 27	320v± 20	0.9735
Haemodynamics						
Mean arterial pressure (mmHg)						
Start	103 ± 22	92 ± 31	75 ± 15	72 ± 29	82 ± 10	**0.0375**
End	130 ± 23	109 ± 33	118 ± 19	98 ± 36	70 ± 54	
Heart rate (beats/min)						
Start	282 ± 44	318 ± 84	315 ± 74	244 ± 53	249 ± 45	0.4207
End	247 ± 85	330 ± 61	326 ± 35	292 ± 50	283 ± 55	
Respiratory variables						
pH						
Start	7.38 ± 0.03	7.48 ± 0.10	7.62 ± 0.15	7.59 ± 0.08	7.47 ± 0.07	**0.0039**
End	7.40 ± 0.06	7.44 ± 0.17	7.65 ± 0.04	7.56 ± 0.08	7.27 ± 0.14	
P_{aCO_2} (mmHg)						
Start	48.8 ± 4.2	33.4 ± 6.3	28.6 ± 15.6	27.8 ± 6.6	39.0 ± 5.8	**0.0173**
End	38.3 ± 10.3	35.3 ± 17.5	18.0 ± 1.7	22.2 ± 3.3	49.1 ± 18.3	
P_{aO_2}/F_{iO_2} (mmHg)						
Start	554 ± 53	510 ± 131	519 ± 116	567 ± 41	551 ± 68	**< 0.0001**
End	665 ± 25	388 ± 150	458 ± 100	493 ± 48	284 ± 261	
Tidal volume (mL)						
Start	1.95 ± 0.08	3.34 ± 0.39	6.84 ± 0.45	8.53 ± 0.61	10.92 ± 1.17	**0.0313**
End	1.95 ± 0.08	3.25 ± 0.68	7.17 ± 0.24	9.20 ± 0.71	10.75 ± 2.27	
Tidal volume (mL/kg)	6.00 ± 0.00	10.44 ± 1.57	21.64 ± 1.27	26.69 ± 2.08	31.56 ± 5.80	**< 0.0001**
Respiratory rate (breaths/min)						
Start	120 ± 4	100 ± 0	60 ± 0	40 ± 0	20 ± 0	0.1012
End	118 ± 4	100 ± 0	60 ± 0	40 ± 0	20 ± 0	
Driving pressure respiratory system (at 6 mL/kg V_T) (cmH_2O)						
Start	4.8 ± 0.9	4.5 ± 0.9	4.2 ± 0.7	4.3 ± 0.7	3.9 ± 0.5	**0.0006**
End	4.7 ± 0.7	5.5 ± 1.9	4.5 ± 0.7	4.0 ± 0.6	9.1 ± 6.1	
Driving pressure lung (cmH_2O)						
Start	4.0 ± 1.0	4.0 ± 0.8	3.6 ± 0.8	3.4 ± 0.6	3.4 ± 0.5	**0.0008**
End	3.8 ± 0.9	4.8 ± 1.9	3.8 ± 0.8	3.1 ± 0.5	8.3 ± 6.1	
Minute ventilation (mL/min)						
Start	233 ± 15	334 ± 39	411 ± 27	341 ± 24	203 ± 40	**0.0163**
End	231 ± 17	325 ± 68	430 ± 15	368 ± 29	195 ± 54	
Alveolar ventilation (mL/min)						
Start	170 ± 13	274 ± 39	375 ± 27	317 ± 24	191 ± 40	**0.0165**
End	184 ± 15	265 ± 68	394 ± 15	344 ± 29	183 ± 54	
Compliance respiratory system (mL/cmH_2O)						
Start	0.42 ± 0.08	0.44 ± 0.07	0.47 ± 0.06	0.46 ± 0.08	0.46 ± 0.11	**0.0003**
End	0.43 ± 0.07	0.39 ± 0.13	0.43 ± 0.07	0.49 ± 0.07	0.29 ± 0.15	
Mechanical power (J/min)						
Start	0.141 ± 0.010	0.093 ± 0.010	0.058 ± 0.004	0.038 ± 0.005	0.021 ± 0.002	**< 0.0001**
End	0.092 ± 0.028	0.099 ± 0.023	0.061 ± 0.014	0.033 ± 0.006	0.027 ± 0.008	

(*Continued*)

© 2025 The Author(s). *The Journal of Physiology* published by John Wiley & Sons Ltd on behalf of The Physiological Society.

14697793, 2026, 3, Downloaded from https://physoc.onlinelibrary.wiley.com/doi/10.1113/JP289904 by Universita Milano Bicocca, Wiley Online Library on [16/03/2026]. See the Terms and Conditions (https://onlinelibrary.wiley.com/terms-and-conditions) on Wiley Online Library for rules of use; OA articles are governed by the applicable Creative Commons License

Table 1. (Continued)

Series 1	Group 0 (DP at 6 mL/kg V_T, RR to reach 140; n = 5)	Group 1 (DP 10, RR 100; n = 8)	Group 2 (DP 20, RR 60; n = 7)	Group 3 (DP 25, RR 40; n = 8)	Group 4 (DP 30, RR 20; n = 8)	P
Lung characteristics						
Water balance (mL)	7.6 ± 3.3	7.8 ± 5.6	10.7 ± 4.3	7.9 ± 3.2	10.3 ± 2.8	0.4197
Wet/dry ratio	5.8 ± 0.5	6.5 ± 0.6	6.5 ± 0.6	7.0 ± 0.6	9.2 ± 2.8	**0.0011**
MicroCT (HU)	−496 ± 65	−424 ± 86	−377 ± 112	−465 ± 115	−208 ± 201	**0.0031**
Gravitational distribution (HU)						
Ventral	−579 ± 29	−511 ± 92	−505 ± 113	−541 ± 83	−314 ± 261	**0.0200**
Dorsal	−424 ± 73	−287 ± 128	−287 ± 110	−377 ± 119	−73 ± 191	**0.0008**
Hypoaerated volume (mL)	0.88 ± 0.29	1.39 ± 0.45	1.51 ± 0.51	1.16 ± 0.44	2.43 ± 1.13	**0.0065**
Alveolar tissue percentage (%)	33 ± 5	35 ± 6	35 ± 6	36 ± 6	48 ± 12	**0.0035**
Inflammatory biomarkers						
BAL poly-morphonuclear cells (%)	14 ± 9	25 ± 17	28 ± 12	44 ± 30	63 ± 19	**0.0006**
BAL proteins (mg/L)	1353 ± 573	2131 ± 1012	1697 ± 911	1792 ± 1555	5233 ± 2480	**0.0114**

P-values shown in bold indicate statistical significance. BAL, broncho-alveolar lavage; bpm: breaths per minute; F_{iO_2}, fraction of inspired oxygen; HU, Hounsfield unit; microCT, micro-computed tomography scan; P_{aCO_2}, partial pressure of carbon dioxide in arterial blood; P_{aO_2}, partial pressure of oxygen in arterial blood; V_T, tidal volume.

volume-controlled mode. After instrumentation, animals were randomly assigned – using a computer-generated randomisation sequence – to one of the two series and, within each series, to one of five ventilatory strategies. Each strategy maintained a constant value of 4DP + RR = 140.

These strategies were divided into five groups:

- Group 0 was ventilated with a tidal volume (V_T) of 6 mL/kg and an initial respiratory rate (RR) of 100 breaths/min. The corresponding driving pressure (DP) was measured under these conditions. Subsequently, RR was adjusted to achieve a target value of 4DP+RR = 140. To account for possible changes in lung mechanics over time, DP was reassessed at the midpoint of the experiment, and RR was modified accordingly to maintain the 4DP+RR target.
- Group 1 with DP = 10 cmH_2O and RR = 100 breaths/min.
- Group 2 with DP = 20 cmH_2O and RR = 60 breaths/min.
- Group 3 with DP = 25 cmH_2O and RR = 40 breaths/min.
- Group 4 with DP = 30 cmH_2O and RR = 20 breaths/min.

Additional ventilatory parameters were standardised, including an inspiratory to expiratory (I/E) ratio of 50%, a positive end-expiratory pressure (PEEP) of 2 cmH_2O, and a fraction of inspired O_2 (F_{iO_2}) of 1.0.

Throughout the experiment, anaesthesia and paralysis were maintained by the infusion of propofol (13 mg/kg/h) and ketamine (5 mg/kg/h) in the right carotid artery and by the infusion of rocuronium bromide (1.5 mg/kg/h) and Ringer–acetate (1.8 mL/h) solution in the right jugular vein. During the administration of the neuromuscular blocking agent, changes in heart rate and blood pressure were continuously monitored and used as reliable indicators of the depth of anaesthesia. Body temperature was maintained between 36 and 37.5°C.

During the protocol, airway pressure (P_{aw}), oesophageal pressure (P_{es}) and haemodynamic parameters were monitored through pressure transducers in the ventilator, at the oesophageal catheter and at the arterial catheter and recorded continuously (LabChart, Version 3.1, ADInstruments, Dunedin, New Zealand).

A recruitment manoeuvre (30 cmH_2O for 10 s) was performed every 60 min, as well as immediately before each measurement of respiratory mechanics and prior to microCT acquisition (Reiss et al., 2011).

Respiratory system (rs) and chest wall (cw) static compliances (C) were evaluated hourly, and arterial blood

© 2025 The Author(s). *The Journal of Physiology* published by John Wiley & Sons Ltd on behalf of The Physiological Society.

14697793, 2026, 3, Downloaded from https://physoc.onlinelibrary.wiley.com/doi/10.1113/JP289904 by Universita Milano Bicocca, Wiley Online Library on [16/03/2026]. See the Terms and Conditions (https://onlinelibrary.wiley.com/terms-and-conditions) on Wiley Online Library for rules of use; OA articles are governed by the applicable Creative Commons License

Table 2. Series 2: HCl-lung-damaged rats undergoing mechanical ventilation for 2 h. Variables assessed in the study were categorised by groups and evaluated at two different time points (start and end). BAL polymorphonuclear cells are expressed as a percentage relative to a total of 200 cells evaluated under the microscope. Data are presented as means ± SD and *P*-values correspond to ordinary one-way ANOVA or Kruskal–Wallis test for variables measured across groups, and to the time × group interaction from a mixed-effects model for variables measured across groups over time (start and end of the experiment). In this experimental series, thirty-one animals were included. The mean weight across all animals was 305 ± 24 g, with no significant differences observed amongst the groups (*P* = 0.8775).

Series 2	Group 0 (DP at 6 mL/kg V_T, RR to reach 140; *n* = 5)	Group 1 (DP 10, RR 100; *n* = 6)	Group 2 (DP 20, RR 60; *n* = 6)	Group 3 (DP 25, RR 40; *n* = 6)	Group 4 (DP 30, RR 20; *n* = 8)	*P*
Body weight (g)	299 ± 17	306 ± 35	316 ± 24	302 ± 23	301 ± 29	0.8775
Haemodynamics						
Mean arterial pressure (mmHg)						
Start	120 ± 34	110 ± 18	96 ± 30	97 ± 31	99 ± 29	**0.0078**
End	101 ± 46	123 ± 14	124 ± 30	117 ± 20	78 ± 26	
Heart rate (beats/min)						
Start	252 ± 64	262 ± 65	259 ± 66	266 ± 33	205 ± 34	**0.0005**
End	157 ± 27	283 ± 46	268 ± 61	268 ± 38	212 ± 65	
Respiratory variables						
pH						
Start	7.38 ± 0.06	7.45 ± 0.12	7.58 ± 0.06	7.56 ± 0.05	7.49 ± 0.05	**0.0003**
End	7.23 ± 0.05	7.46 ± 0.04	7.54 ± 0.06	7.38 ± 0.13	7.30 ± 0.08	
P_{aCO_2} (mmHg)						
Start	46.3 ± 5.8	36.3 ± 12.1	25.6 ± 3.6	29.8 ± 4.1	37.0 ± 5.5	0.1033
End	55.7 ± 18.6	32.6 ± 3.4	23.9 ± 3.4	41.3 ± 14.8	36.6 ± 11.6	
P_{aO_2}/F_{iO_2} (mmHg)						
Start	538 ± 97	555 ± 50	547 ± 51	572 ± 21	573 ± 43	< **0.0001**
End	346 ± 204	516 ± 46	361 ± 106	251 ± 190	122 ± 76	
Tidal volume (mL)						
Start	1.80 ± 0.10	2.83 ± 0.85	6.48 ± 0.37	8.35 ± 0.62	10.78 ± 0.92	< **0.0001**
End	1.80 ± 0.10	2.92 ± 0.39	5.82 ± 0.66	6.28 ± 1.34	10.45 ± 0.88	
Tidal volume (mL/kg)	6.00 ± 0.00	9.24 ± 2.66	20.56 ± 0.68	27.80 ± 2.67	37.22 ± 4.12	< **0.0001**
Respiratory rate (breaths/min)						
Start	122 ± 3	100 ± 0	60 ± 0	40 ± 0	20 ± 0	< **0.0001**
End	114 ± 9	100 ± 0	60 ± 0	40 ± 0	20 ± 0	
Driving pressure respiratory system (at 6 mL/kg V_T) (cmH_2O)						
Start	4.7 ± 0.7	3.8 ± 0.3	4.1 ± 0.5	4.2 ± 0.6	3.8 ± 0.6	< **0.0001**
End	7.8 ± 1.1	4.7 ± 0.7	5.7 ± 0.7	9.1 ± 3.4	12.2 ± 5.5	
Driving pressure lung (cmH_2O)						
Start	3.7 ± 0.6	3.3 ± 0.3	3.4 ± 0.4	3.5 ± 0.6	3.4 ± 0.6	< **0.0001**
End	6.7 ± 1.3	4.1 ± 0.8	5.0 ± 0.8	8.3 ± 3.4	11.7 ± 5.5	
Minute ventilation (mL/min)						
Start	219 ± 14	283 ± 85	389 ± 22	334 ± 25	223 ± 21	**0.0008**
End	206 ± 25	292 ± 39	349 ± 40	251 ± 54	213 ± 19	
Alveolar ventilation (mL/min)						
Start	185 ± 13	223 ± 85	353 ± 22	310 ± 25	211 ± 21	**0.0007**
End	160 ± 21	232 ± 39	313 ± 40	227 ± 54	201 ± 19	
Compliance respiratory system, mL/cmH_2O						
Start	0.39 ± 0.07	0.48 ± 0.05	0.47 ± 0.03	0.44 ± 0.06	0.49 ± 0.09	**0.0002**
End	0.24 ± 0.05	0.40 ± 0.07	0.34 ± 0.05	0.22 ± 0.08	0.19 ± 0.11	
Mechanical power (J/min)						
Start	0.113 ± 0.024	0.103 ± 0.015	0.063 ± 0.011	0.038 ± 0.005	0.020 ± 0.004	0.3306
End	0.127 ± 0.024	0.091 ± 0.011	0.083 ± 0.059	0.048 ± 0.010	0.036 ± 0.013	

(*Continued*)

© 2025 The Author(s). *The Journal of Physiology* published by John Wiley & Sons Ltd on behalf of The Physiological Society.

14697793, 2026, 3, Downloaded from https://physoc.onlinelibrary.wiley.com/doi/10.1113/JP289904 by Universita Milano Bicocca, Wiley Online Library on [16/03/2026]. See the Terms and Conditions (https://onlinelibrary.wiley.com/terms-and-conditions) on Wiley Online Library for rules of use; OA articles are governed by the applicable Creative Commons License

Table 2. (Continued)

Series 2	Group 0 (DP at 6 mL/kg V_T, RR to reach 140; n = 5)	Group 1 (DP 10, RR 100; n = 6)	Group 2 (DP 20, RR 60; n = 6)	Group 3 (DP 25, RR 40; n = 6)	Group 4 (DP 30, RR 20; n = 8)	P
Lung characteristics						
Water balance (mL)	6.0 ± 1.8	5.7 ± 2.4	6.3 ± 1.1	6.6 ± 0.7	5.7 ± 2.1	0.9049
Wet/dry ratio	7.1 ± 1.1	6.3 ± 0.9	7.6 ± 1.1	9.3 ± 1.8	13.1 ± 3.8	**0.0008**
MicroCT (HU)	−338 ± 122	−342 ± 192	−240 ± 85	−106 ± 115	88 ± 74	**0.0018**
Gravitational distribution (HU)						
Ventral	−527 ± 62	−463 ± 176	−517 ± 35	−377 ± 116	−2 ± 135	**0.0008**
Dorsal	−222 ± 139	−272 ± 169	−139 ± 95	30 ± 125	150 ± 59	**0.0028**
Hypoaerated volume (mL)	1.77 ± 0.65	1.53 ± 0.66	2.43 ± 0.38	2.63 ± 0.71	4.54 ± 0.62	**0.0149**
Alveolar tissue percentage (%)	37 ± 8	38 ± 7	42 ± 5	47 ± 6	61 ± 11	**< 0.0001**
Inflammatory biomarkers						
BAL polymorphonuclear cells (%)	13 ± 6	18 ± 18	54 ± 19	46 ± 26	57 ± 16	**0.0003**
BAL proteins (mg/L)	1841 ± 909	2329 ± 1099	4035 ± 1039	5104 ± 1411	6352 ± 1641	**< 0.0001**

P-values shown in bold indicate statistical significance. BAL, broncho-alveolar lavage; bpm: breaths per minute; F_{iO_2}, fraction of inspired oxygen; HU, Hounsfield unit; microCT, micro-computed tomography scan; P_{aCO_2}, partial pressure of carbon dioxide in arterial blood; P_{aO_2}, partial pressure of oxygen in arterial blood; V_T, tidal volume.

gas analysis was performed at the beginning, in the middle and at the end of the experiment.

A lung microCT scan was performed *in vivo* at the end of the experiment, during volume-controlled ventilation with a V_T of 6 mL/kg and a fixed RR of 100 breaths/min, to estimate lung density by Hounsfield units (HU).

A broncho-alveolar lavage (BAL) was performed after euthanasia through the endotracheal tube, collecting fluid from both lungs. A total of 15 mL of phosphate-buffered saline (PBS) was instilled in three separate aliquots of 5 mL each. BAL fluid was then recovered, centrifuged and the supernatant was snap frozen and stored at −80°C. Total protein concentrations in the BAL fluid were subsequently measured.

At the end of the experiment, animals were killed by exsanguination under anaesthesia.

Finally, the lungs were dissected from the thorax. The middle right lobe was removed for the evaluation of wet/dry (W/D) ratio, whilst the upper right lobe was isolated and fixed for the histological evaluation of lung damage, using quantitative stereological techniques.

Lung-injury protocol

Lung injury was induced by intratracheal instillation of HCl at a concentration of 0.1 M, administered in a quantity of 1 mL per kilogram of body weight through the endotracheal tube immediately following intubation. The rats were maintained supine in anti-Trendelenburg position (45° angle) for 10 min, after which they were positioned flat (0° angle) and ventilated according to the assigned ventilation group.

Calculation of alveolar ventilation

For the calculation of alveolar ventilation (VA), the approach described by Dassow et al. (2013) was followed. In their study, the authors calculated the dead space of similar mean weight using a small-animal CO_2 sensor based on infrared absorption at three different levels of V_T. A dead space of 0.4 mL was applied for groups ventilated at 6 mL/kg, whilst a value of 0.6 mL was used for groups ventilated with 8 mL/kg or greater.

Oesophageal pressure

Throughout the experiment, P_{es} was continuously monitored using an oesophageal catheter designed for small animals (Pressure Catheter 3.5F, SPR-524, Millar). To verify the correct positioning of the oesophageal catheter, a Baydur test was performed. During an end-expiratory airway occlusion in controlled mechanical ventilation, three gentle compressions on the chest should generate similar positive deflections in P_{aw} and P_{es} with $\Delta P_{aw}/\Delta P_{es}$ ratio ideally equal to 1 (Baydur et al., 1982; Docci et al., 2025).

DP of the lung (L) was calculated as the difference between the DP_{rs} and the DP_{cw}. DP_{cw} was determined as the difference between the P_{es} at the end of inspiration

© 2025 The Author(s). *The Journal of Physiology* published by John Wiley & Sons Ltd on behalf of The Physiological Society.

14697793, 2026, 3, Downloaded from https://physoc.onlinelibrary.wiley.com/doi/10.1113/JP289904 by Universita Milano Bicocca, Wiley Online Library on [16/03/2026]. See the Terms and Conditions (https://onlinelibrary.wiley.com/terms-and-conditions) on Wiley Online Library for rules of use; OA articles are governed by the applicable Creative Commons License

and expiration, measured during an end-inspiratory and end-expiratory hold (Akoumianaki et al., 2014).

Calculation of mechanical power

The mechanical power (MP) was calculated using the formula for volume-controlled ventilation derived from the work of Chiumello et al. (2020):

$$\begin{aligned} MP &= 0.098 \times RR \times \text{tidal volume} \\ &\times \text{Peak inspiratory pressure} \\ &- 1/2 \left(\text{Plateau pressure} - PEEP\right) \end{aligned}$$

where 0.098 is a conversion factor from $cmH_2O\ L\ min^{-1}$ in J/min.

MicroCT scan

Lung microCT scan was performed at the end of the experiment using microCT machine (Skyscan 1176, Bruker, Billerica, MA, USA), with rats undergoing mechanical ventilation with a V_T of 6 mL/kg.

For the reconstruction, NRECON, version 1.6.9.4, Skyscan software was used, transforming 2D projection images into 3D volumes. For the analysis, Dataviewer, version 1.7.0.1, Skyscan segmentation software was used, which exploits a slice-by-slice inspection of 3D volumes and 2D/3D image registration.

For the comparisons, the mean Hounsfield unit (HU) value was calculated across both lungs. Additionally, a CT analysis was performed by dividing the image into dorsal and ventral parts, based on gravitational orientation, and averaging these regions across both lungs (Magliocca et al., 2021; Magliocca et al., 2024; Rezoagli et al., 2022). Finally, quantitative gas volume analysis was performed using dedicated software. Regions of interest (ROIs) were manually defined to include the entire lung parenchyma in each axial microCT slice. Within each ROI, the software automatically segmented lung tissue based on predefined greyscale attenuation thresholds, classifying voxels into normally aerated, poorly aerated and non-aerated compartments. The volumetric contribution of each compartment was calculated by summing the voxel volumes across all slices. This approach allowed for precise quantification of aeration patterns across the lung, enabling assessment of regional ventilation and detection of hypoaerated or consolidated areas. The percentage of each compartment relative to the total lung volume was also derived to allow inter-subject comparison.

BAL polymorphonuclear cells count

A polymorphonuclear cell (PMN) count was performed using a manual cell counting method. A small volume of BAL with cell suspension was loaded over a thick glass microscope slide. After counting 200 cells using a light microscope, the concentration of PMNs in the original suspension was calculated.

Protein concentration evaluation

A portion of BAL was stored at −80°C for the subsequent evaluation of protein concentrations quantified by the bicinchoninic acid assay (BCA assay; Thermo Fisher Scientific, Waltham, MA, USA) according to the manufacturer's instructions.

Histological analysis

Preparation of lung tissue. The upper lobe of the right lung was isolated and fixed for morphometric analysis: it was stored in paraformaldehyde for 24 h and then embedded in paraffin wax. Following fixation, the vertical axis was identified and the lobe was sliced into three equal sections, each 4 mm thick, perpendicular to this axis using a sharp blade.

Paraffin embedding. After sectioning the paraformaldehyde-fixed lung lobe, the sections were placed in a labelled histoprocessing cassette (Sigma-Aldrich, Burlington, MA, USA), with details of the animal inscribed by pencil. These sections were then processed in a histoprocessor (ASP 300 histoprocessor, Leica Microsystems, Wetzlar, Germany) and retrieved the next morning. Paraffin wax embedding was carried out using a Heated Paraffin Embedding Module (Leica).

Slide preparation. Sections were cut at 7 μm using a microtome (Leica RM2235 Microtome). Each section was carefully inspected on the surface of water maintained at 40°C for any imperfections before being transferred onto Superfrost Plus microscope slides (Thermo Scientific) and allowed to drain. The sections were stored at room temperature overnight before proceeding to staining with haematoxylin and eosin.

Haematoxylin and eosin histological staining. The following day, the slides underwent deparaffinisation and rehydration through two xylene baths and graded alcohols (100%, 90% and 70%, respectively), followed by a 2-min rinse with running tap water. Subsequently, the slides were placed in a bath of haematoxylin for 6 min and rinsed for 4 min under running tap water. After checking for adequate staining, eosin staining was carried

© 2025 The Author(s). The Journal of Physiology published by John Wiley & Sons Ltd on behalf of The Physiological Society.

14697793, 2026, 3, Downloaded from https://physoc.onlinelibrary.wiley.com/doi/10.1113/JP289904 by Universita Milano Bicocca, Wiley Online Library on [16/03/2026]. See the Terms and Conditions (https://onlinelibrary.wiley.com/terms-and-conditions) on Wiley Online Library for rules of use; OA articles are governed by the applicable Creative Commons License

out for 2 min, followed by dehydration through alcohol baths of varying concentrations (50%, 70%, 95% and 100%) for 30 s each. The slides were then immersed in eosin for 2 min and subjected to two xylene baths, each lasting 15 min. Finally, the slides were mounted in DPX mountant (VWR International, Ballycoolin, Ireland) and coverslipped (Thermo Scientific Thickness: No. 1). The mounted slides were left overnight at room temperature to allow DPX mountant to spread between the sections and the cover slips. Slides prepared in this manner were stored in plastic slide boxes at room temperature, shielded from light.

Stereological analysis. A quantitative stereological technique, as described by Hopkins et al. (2001), was performed. Slides prepared as described above were examined at ×100 magnification under a microscope with a bright field view (Leica BioSystem, Aperio digital pathologyslide scanner, ScanScope, Leica Microsystems Srl, Milano, Italy). Six randomly chosen fields of view from each slide were digitised using a digital camera (Olympus BX61, Mason technologies, Milan, Italy). Images were stored in eight-bit format. The x and y grid coordinates for each image were recorded using the scale attached to the microscope (200 μm). A 100-point counting grid was overlaid on each image using ImageJ imaging software package (Version 1.52k, Wayne Rashband, NIH, Bethesda, MD, USA). A touch count was performed at each of the 100 intersection points on the grid, recording acinar tissue, non-acinar tissue and airspace. Intra-acinar tissue was defined as all tissues within the gas exchange portion of the lung, including respiratory bronchioles, alveolar ducts, alveolar sacs and alveoli, along with blood vessels within their walls. The intra-acinar airspace was defined as all airspaces within the lumen of respiratory bronchioles, alveolar ducts, alveolar sacs and alveoli. Intersections of the grid were manually counted for airspace, acinar and non-acinar tissue, with non-acinar tissue subtracted from the overall tissue to determine the percentage of alveolar tissue.

Statistical analysis and sample size. Continuous variables were tested for normal distribution with the Kolmogorov–Smirnov test and are presented as mean ± standard deviation (SD). Differences in variances between groups were assessed by one-way analysis of variance (ANOVA) or by the Kruskal–Wallis test, based on distribution. *Post hoc* multiple comparisons between groups were performed by the Benjamini, Krieger and Yekutieli (BKY) method. P-values <0.05 (two-tailed) were considered statistically significant. Differences amongst groups over time were tested using a mixed-effects model with fixed effects for time (i.e., start and end of experiment), group (0-1-2-3-4), and their interaction, and a random effect for rat ID. Time × group interaction P-values were reported in both Series 1 and 2.

Correlations between continuous variables were explored by linear regression analyses in both Series 1 and 2. Robust clustering was implemented to adjust the models for the within-animal correlation by considering the animals as the cluster variable.

Statistical analysis was performed using the software GraphPad Prism (Version 9.5.1, GraphPad Software, Boston, MA, USA) and R (cran.r-project.org).

The sample size was determined based on the reduction principle of the 3Rs (Díaz et al., 2020), on previous experience with this experimental model, and supported by published investigations on the topic (Horie et al., 2021; Moraes et al., 2018; Pecchiari et al., 2014; Zambelli et al., 2023). To ensure adequate statistical power, a minimum of five animals per group was included.

Results

Haemodynamic and respiratory variables

Mean arterial pressure (MAP) changed over time, with a significant time × group interaction ($P = 0.0375$; Table 1). Heart rate (HR) did not differ significantly between the start and end of the experiment (time × group interaction $P = 0.4207$; Table 1).

After 4 h of mechanical ventilation, group 4, which had the highest DP and lowest RR, showed a significant decrease in P_{aO_2}/F_{iO_2} (284 ± 261 mmHg; Fig. 2*A*) and in C_{rs} (0.29 ± 0.15 mL/cmH_2O; Fig. 2*D*) compared to the other groups in *post hoc* comparisons (all adjusted $P < 0.05$). The change in P_{aCO_2} and pH across groups (Fig. 2*B* and Table 1) followed the changes in VA (Fig. 2*C*) according to the combination of DP and RR to keep 4DP+RR constant.

Lung characteristics and inflammatory biomarkers

Lung oedema, assessed by the W/D ratio (Fig. 2*E*), was more pronounced in Group 4 (9.2 ± 2.8), resulting in the highest lung density amongst all groups in *post hoc* comparisons, as assessed by microCT scans (−208 ± 201 HU); Fig. 2*F*) (all BKY $P < 0.05$).

Furthermore, the percentage of PMNs in BAL increased as DP levels rose and RR decreased, with Group 3 and 4 showing higher counts (44 ± 30% and 63 ± 19% respectively, Fig. 2*G*). BAL proteins exhibited a threshold effect at DP equal to 30 cmH_2O, with Group 4 showing a significant higher value compared to the other groups in *post hoc* comparisons (5233 ± 2480 mg/L, all adjusted $P < 0.05$; Fig. 2*H*)

© 2025 The Author(s). *The Journal of Physiology* published by John Wiley & Sons Ltd on behalf of The Physiological Society.

14697793, 2026, 3, Downloaded from https://physoc.onlinelibrary.wiley.com/doi/10.1113/JP289904 by Universita Milano Bicocca, Wiley Online Library on [16/03/2026]. See the Terms and Conditions (https://onlinelibrary.wiley.com/terms-and-conditions) on Wiley Online Library for rules of use; OA articles are governed by the applicable Creative Commons License

Partitioned respiratory mechanics and lung aeration

The percentage of hypoaerated lung volume was significantly higher in Group 4 compared to the other groups in *post hoc* comparisons (46.5 ± 19.5%, all BKY $P < 0.05$; Fig. 3*A*). Similarly, driving pressure of the lung (DP_L), at the end of the experiment, showed a trend towards higher values in Group 4 (8.3 ± 6.1 cmH_2O; Fig. 3*B*). A strong positive correlation was found between DP_L and hypoaerated lung volume, indicating that an increased extent of lung hypoaeration was positively associated with higher DP_L values ($r = 0.71$, $P = 0.0004$; Fig. 3*C*).

Mechanical power and lung aeration

MP, at the end of the experiment, was significantly lower in Group 3 and 4 compared to the other groups in *post hoc* comparisons (0.033 ± 0.006 and 0.027 ± 0.008 J/min, respectively, all adjusted $P < 0.05$; Fig. 4*B*). A negative correlation was found between MP and hypoaerated lung volume, suggesting that MP values were not associated with a greater extent of lung hypoaeration ($r = 0.19$, $P = 0.5488$; Fig. 4*C*). A correlation between MP and alveolar tissue percentage was tested but was not significant ($r = 0.24$, $P = 0.2812$).

Gravitational distribution of lung density at microCT scan and histological evaluation

MicroCT scan analysis revealed an increase in lung density as DP increased and RR decreased, measured as the mean HU in both lungs (Fig. 2*F*). Representative CT scan images (Fig. 5*A* and *B*) illustrate this trend.

Further analysis of the gravitational distribution of lung density demonstrated a significantly higher density in the dorsal lung zones compared to the ventral lung zones ($P < 0.0001$; Fig. 5*E*). Notably, Group 4 exhibited a significant higher density in both ventral (−314 ± 261 HU) and dorsal (−73 ± 191 HU) regions compared to all other groups in *post hoc* comparisons (all BKY $P < 0.05$)

Representative histological sections (Fig. 5*C* and *D*), obtained from the same animals shown in the CT scans, confirm these findings, showing an increased mean alveolar tissue percentage (Fig. 5*F*), evaluated using stereological techniques, following the same trend as observed in microCT scans.

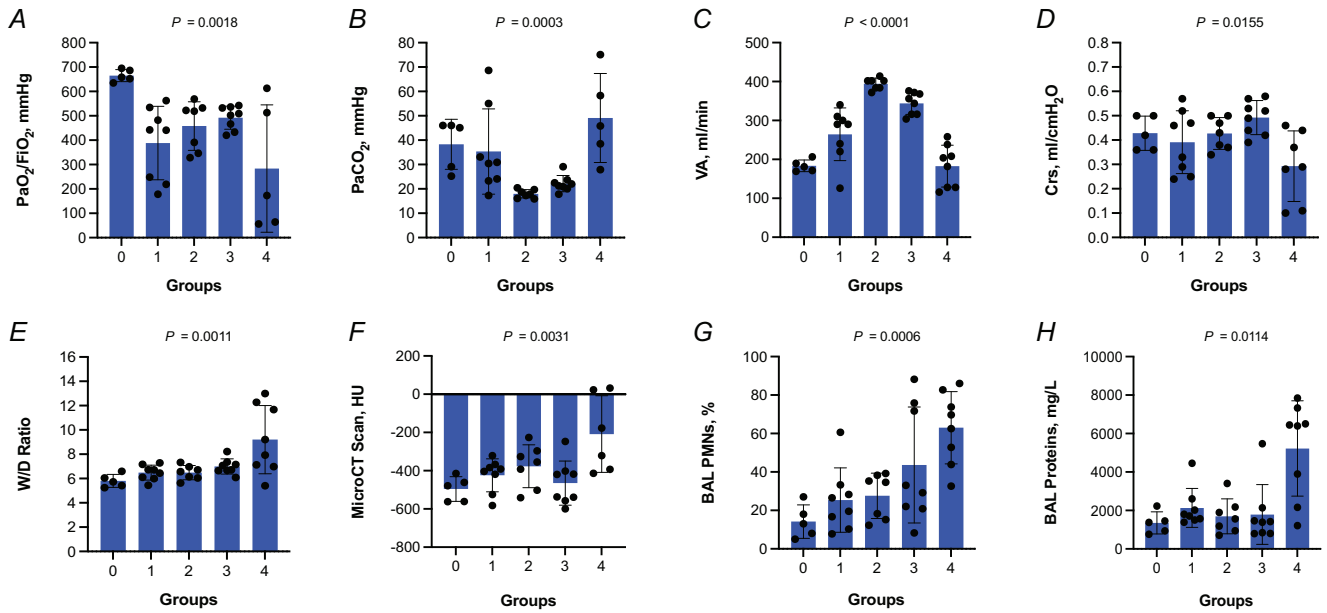

Figure 2.
P_{aO_2}/F_{iO_2} ratio (*A*), P_{aCO_2} (*B*), VA (*C*), C_{rs} (*D*), W/D ratio (*E*), microCT scan (*F*), BAL PMNs (*G*) and BAL proteins (*H*) in healthy rats undergoing mechanical ventilation for 4 h (Series 1). P_{aO_2}/F_{iO_2} ratio, P_{aCO_2}, VA and C_{rs} were assessed at the end of the experiment. BAL PMNs are represented as a percentage relative to a total of 200 cells evaluated under the microscope. Bars represent the mean, error bars represent SD, and each dot represents an individual animal. *P*-values correspond to ordinary one-way ANOVA or Kruskal–Wallis test. n = 5–8 animals per group. Abbreviations: BAL, broncho-alveolar lavage; C_{rs}, respiratory system compliance; F_{iO_2}, fraction of inspired oxygen; HU, Hounsfield unit; microCT, micro-computed tomography scan; P_{aCO_2}, partial pressure of carbon dioxide in arterial blood; P_{aO_2}, partial pressure of oxygen in arterial blood; PMNs, polymorphonuclear cells; VA, alveolar ventilation; W/D, wet to dry ratio.

© 2025 The Author(s). *The Journal of Physiology* published by John Wiley & Sons Ltd on behalf of The Physiological Society.

14697793, 2026, 3, Downloaded from https://physoc.onlinelibrary.wiley.com/doi/10.1113/JP289904 by Universita Milano Bicocca, Wiley Online Library on [16/03/2026]. See the Terms and Conditions (https://onlinelibrary.wiley.com/terms-and-conditions) on Wiley Online Library for rules of use; OA articles are governed by the applicable Creative Commons License

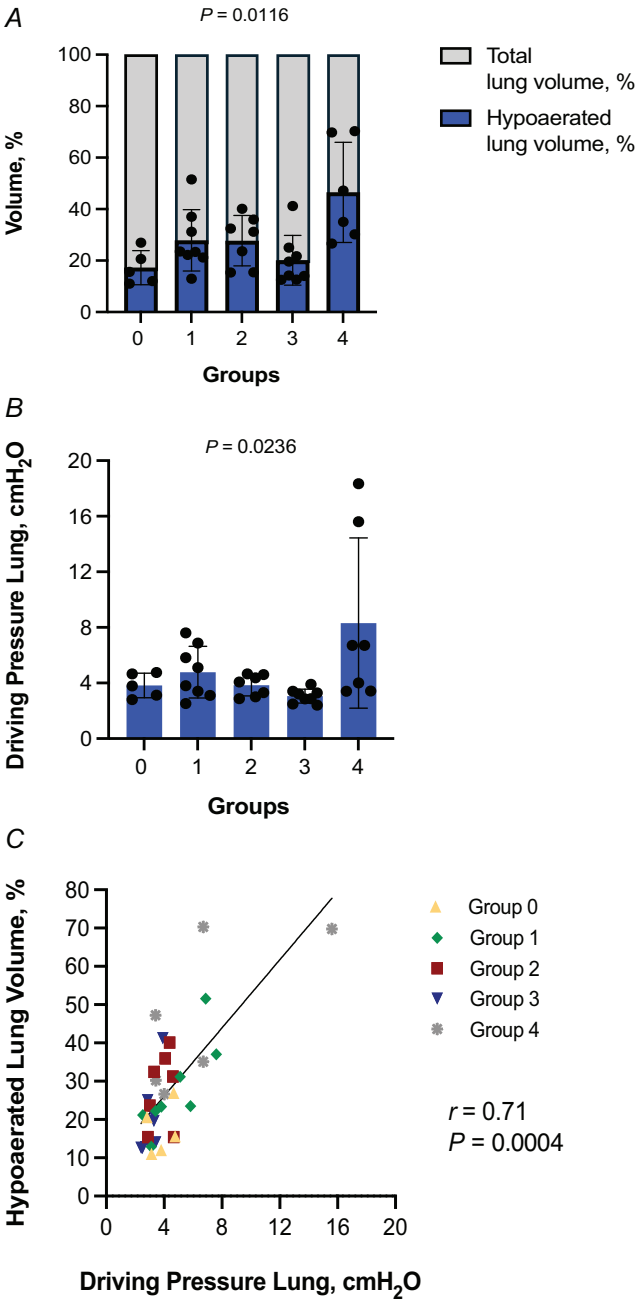

Figure 3.
Graphical representation of percentage of hypoaerated lung volume relative to total lung volume assessed by microCT (*A*); DP_L evaluated with 6 mL/kg of V_T (*B*) and correlation between DP_L and hypoaerated lung volume in individual animals (*C*). Bars represent the mean, error bars represent SD, and each dot represents an individual animal. *P*-values (*A* and *B*) correspond to ordinary one-way ANOVA or Kruskal–Wallis test. Pearson correlation coefficient (*r*) with corresponding *P*-value is shown in panel *C*. *n* = 5–8 animals per group. DP_L: driving pressure of the lung.

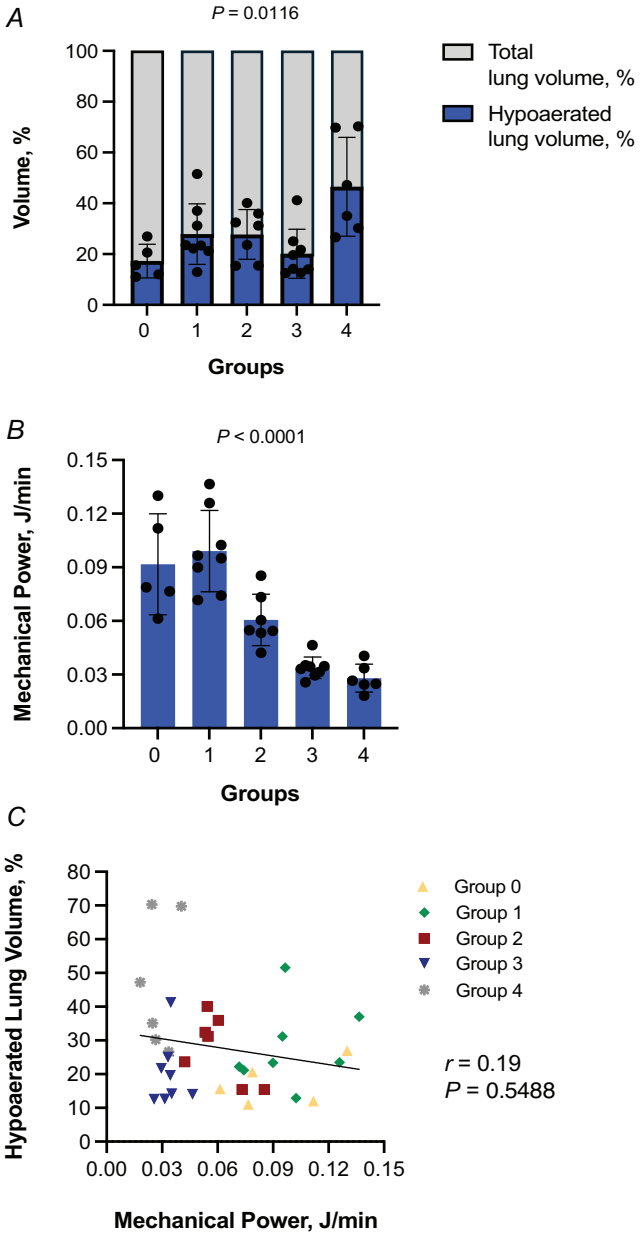

Figure 4.
Graphical representation of percentage of hypoaerated lung volume relative to total lung volume assessed by microCT (A), mechanical power (B) and correlation between mechanical power and hypoaerated lung volume in individual animals (C). Bars represent the mean, error bars represent SD, and each dot represents an individual animal. *P*-values (*A* and *B*) correspond to ordinary one-way ANOVA or Kruskal–Wallis test. Pearson correlation coefficient (*r*) with corresponding *P*-value is shown in panel *C*. *n* = 5–8 animals per group. MP: mechanical power.

© 2025 The Author(s). *The Journal of Physiology* published by John Wiley & Sons Ltd on behalf of The Physiological Society.

14697793, 2026, 3, Downloaded from https://physoc.onlinelibrary.wiley.com/doi/10.1113/JP289904 by Universita Milano Bicocca, Wiley Online Library on [16/03/2026]. See the Terms and Conditions (https://onlinelibrary.wiley.com/terms-and-conditions) on Wiley Online Library for rules of use; OA articles are governed by the applicable Creative Commons License

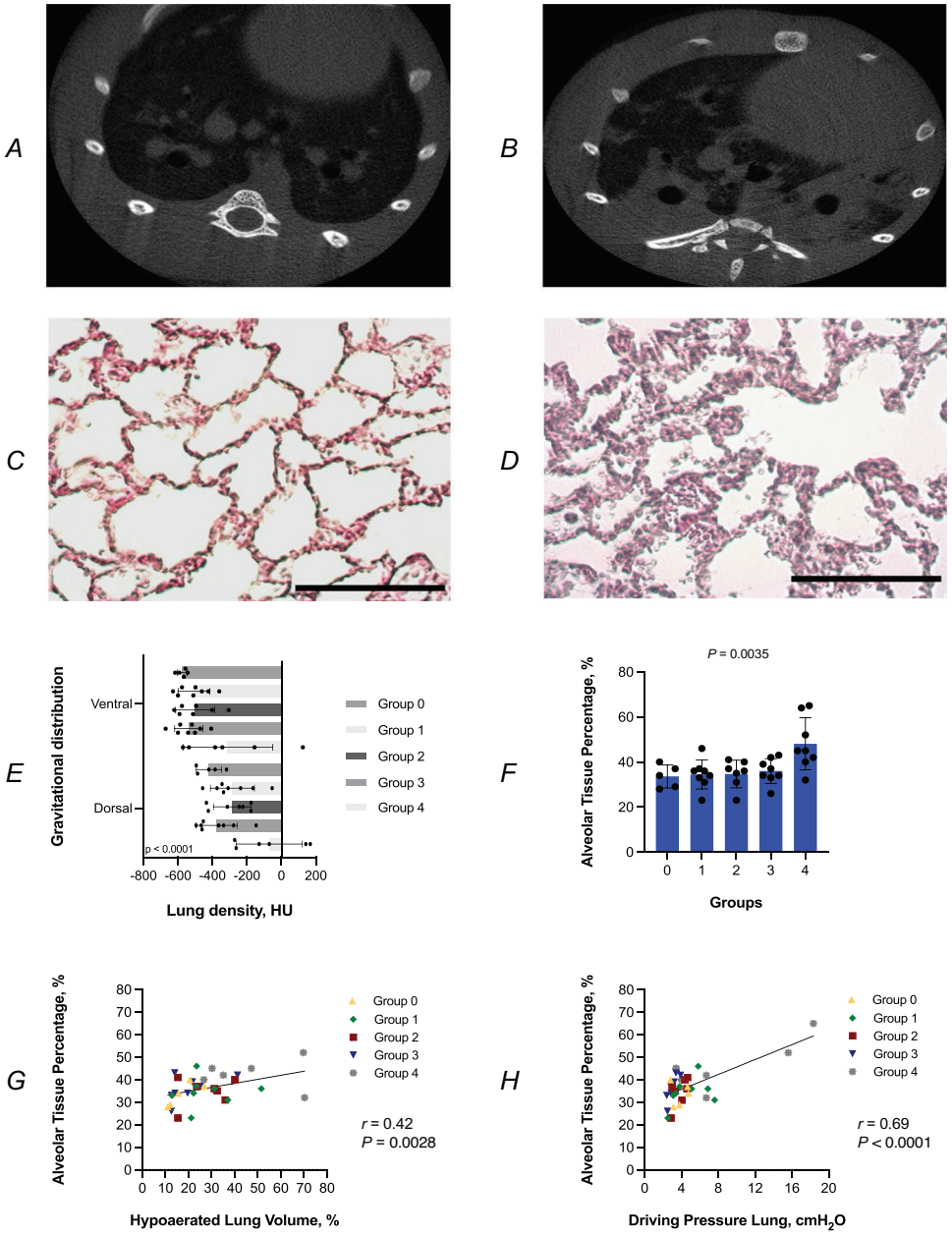

Figure 5.
Representative CT images for Group 0 (*A*) and Group 4 (*B*); representative histological sections from the same animals for Group 0 (*C*) and Group 4 (*D*); lung density variations across different gravitational levels in ventral and dorsal lung areas across groups (*E*); mean alveolar tissue percentage (*F*); correlation between hypoaerated lung volume and alveolar tissue percentage (*G*); correlation between DP_L and alveolar tissue percentage (*H*). For lung histology images, scale bar = 100 µm. Bars represent the mean, error bars represent SD, and each dot represents an individual animal. *P*-values (*E*-*F*) correspond to ordinary one-way ANOVA or Kruskal–Wallis test. Pearson correlation coefficients (*r*) with corresponding *P*-values are reported in panels *G* and *H*. *n* = 5–8 animals per group.

© 2025 The Author(s). *The Journal of Physiology* published by John Wiley & Sons Ltd on behalf of The Physiological Society.

14697793, 2026, 3, Downloaded from https://physoc.onlinelibrary.wiley.com/doi/10.1113/JP289904 by Universita Milano Bicocca, Wiley Online Library on [16/03/2026]. See the Terms and Conditions (https://onlinelibrary.wiley.com/terms-and-conditions) on Wiley Online Library for rules of use; OA articles are governed by the applicable Creative Commons License

A strong positive correlation was found between hypoaerated lung volume and alveolar tissue percentage ($r = 0.42$, $P = 0.0028$, Fig. 5*G*), and between DP_L and alveolar tissue percentage ($r = 0.69$, $P < 0.0001$, Fig. 5*H*).

Haemodynamic and respiratory variables

Both MAP and HR changed over time, with significant time × group interactions ($P = 0.0078$ and $P = 0.0005$, respectively; Table 2).

After 2 h of mechanical ventilation, Group 4, characterised by the highest DP and the lowest RR, exhibited a significant decrease in P_{aO_2}/F_{iO_2} (122 ± 76 mmHg; Fig. 6*A*) compared to the other groups in *post hoc* comparisons (all BKY $P < 0.05$). Additionally, C_{rs} was significantly lower in Group 3 and 4 (0.22 ± 0.08 and 0.19 ± 0.11 mL/cmH_2O, respectively) compared to all other groups in *post hoc* comparisons, except for Group 0 (BKY $P < 0.05$; Fig. 6*D*). The P_{aCO_2} trend (Fig. 6*B*) followed changes in VA (Fig. 6*C*), as ventilation was adjusted to maintain a fixed 4DP+RR value. This was further corroborated by arterial pH measurements (Table 2).

Lung characteristics and inflammatory biomarkers

Lung oedema, assessed by the W/D ratio (Fig. 6*E*), was significantly higher in Group 4 (13.1 ± 3.8), resulting in the highest lung density amongst all groups in *post hoc* comparisons as evaluated by microCT scans (88 ± 74 HU, all adjusted $P < 0.05$; Fig. 6*F*). This occurred independently of water balance ($P = 0.9049$; Table 2).

The percentage of PMNs in BAL demonstrated a threshold effect at DP equal to 20 cmH_2O, with Groups 2, 3 and 4 showing values of 54 ± 19%, 46 ± 26% and 57 ± 16%, respectively (Fig. 6*G*). BAL proteins increased with rising DP and decreasing RR (Fig. 6*H*).

Partitioned respiratory mechanics and lung aeration

The percentage of hypoaerated lung volume was significantly higher in Group 4 compared to the other groups (except for Group 3) in *post hoc* comparisons (77.0 ± 5.2%, BKY $P < 0.05$; Fig. 7*A*). Similarly, DP_L, at the end of the experiment, was significantly higher in Group 4 amongst all groups in *post hoc* comparisons (11.7 ± 5.5 cmH_2O, all adjusted $P < 0.05$; Fig. 7*B*). A strong positive correlation was found between DP_L and hypoaerated lung volume, indicating that an increased

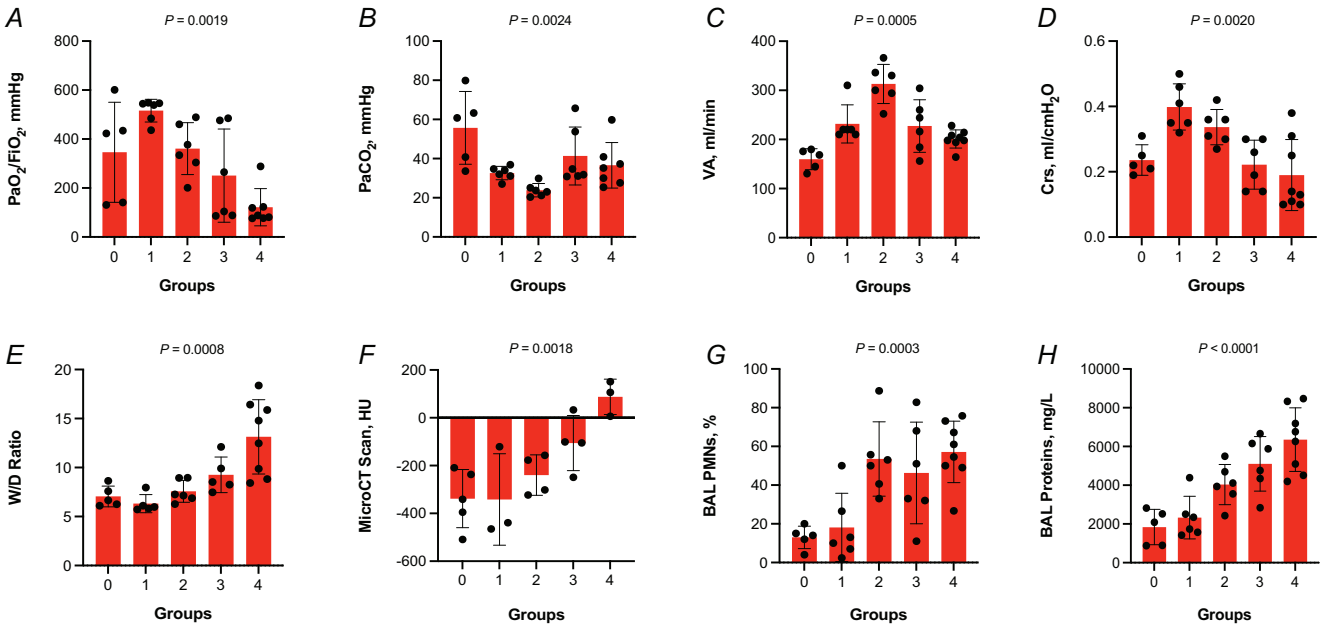

Figure 6.
P_{aO_2}/F_{iO_2} ratio (*A*), P_{aCO_2} (*B*), VA (*C*), C_{rs} (*D*), W/D ratio (*E*), microCT scan (*F*), BAL PMNs (*G*) and BAL proteins (*H*) in lung-damaged rats undergoing mechanical ventilation for 2 h (Series 2). P_{aO_2}/F_{iO_2} ratio, P_{aCO_2}, VA and C_{rs} were assessed at the end of the experiment. BAL PMNs are represented as a percentage relative to a total of 200 cells evaluated under the microscope. Bars represent the mean, error bars represent SD, and each dot represents an individual animal. *P*-values correspond to ordinary one-way ANOVA or Kruskal–Wallis test. The number of animals per group ranged from 3 to 8 (n = 3–8). BAL, broncho-alveolar lavage; C_{rs}, respiratory system compliance; F_{iO_2}, fraction of inspired oxygen; HU, Hounsfield unit; microCT, micro-computed tomography scan; P_{aCO_2}, partial pressure of carbon dioxide in arterial blood; P_{aO_2}, partial pressure of oxygen in arterial blood; PMNs, polymorphonuclear cells; VA, alveolar ventilation; W/D, wet to dry ratio.

© 2025 The Author(s). *The Journal of Physiology* published by John Wiley & Sons Ltd on behalf of The Physiological Society.

14697793, 2026, 3, Downloaded from https://physoc.onlinelibrary.wiley.com/doi/10.1113/JP289904 by Universita Milano Bicocca, Wiley Online Library on [16/03/2026]. See the Terms and Conditions (https://onlinelibrary.wiley.com/terms-and-conditions) on Wiley Online Library for rules of use; OA articles are governed by the applicable Creative Commons License

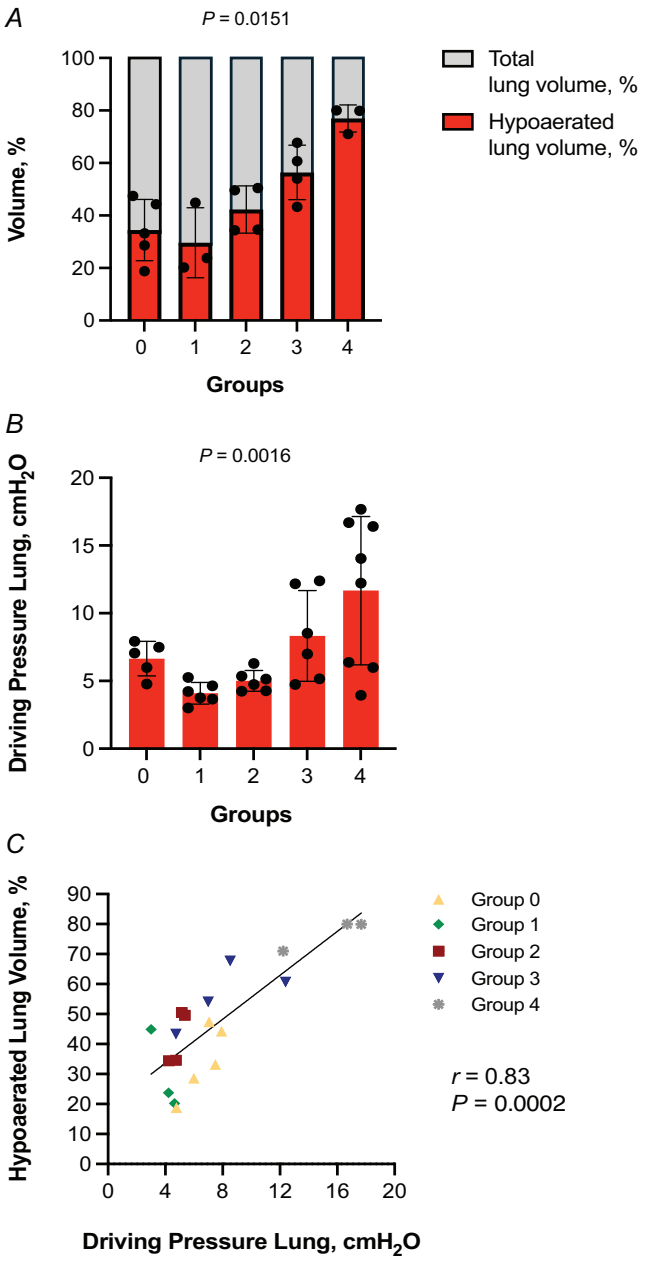

Figure 7.
Graphical representation of percentage of hypoaerated lung volume relative to total lung volume assessed by microCT (*A*), DP_L evaluated with 6 mL/kg of V_T (*B*) and correlation between DP_L and hypoaerated lung volume in individual animals (*C*). Bars represent the mean, error bars represent SD, and each dot represents an individual animal. *P*-values (*A* and *B*) correspond to ordinary one-way ANOVA or Kruskal–Wallis test. Pearson correlation coefficient (*r*) with corresponding *P*-value is shown in panel *C*. *n* = 3–8 animals per group. DP_L, driving pressure of the lung.

extent of lung hypoaeration was positively associated with higher DP_L values ($r = 0.83$, $P = 0.0002$; Fig. 7*C*).

Mechanical power and lung aeration

MP, at the end of the experiment, was significantly lower in Group 4 compared to other groups (except for Group 3) in *post hoc* comparisons (0.036 ± 0.013 J/min, BKY $P < 0.05$; Fig. 8*B*). A negative correlation was found between MP and hypoaerated lung volume, suggesting that MP values were not associated with a greater extent of lung hypoaeration ($r = 0.30$, $P = 0.2456$; Fig. 8*C*). A correlation between MP and alveolar tissue percentage was tested but was not significant ($r = 0.57$, $P = 0.0771$).

Gravitational distribution of lung density at microCT scan and histological evaluation

MicroCT scans revealed increased lung density as DP increased and RR decreased, measured as the mean HU in both lungs (Fig. 6*F*). Representative CT scan images (Fig. 9*A* and *B*) illustrate this trend.

Further analysis of the gravitational distribution of lung density demonstrated a significantly higher density in the dorsal lung zones compared to the ventral lung zones ($P < 0.0001$; Fig. 9*E*).

Notably, Group 4 exhibited a significantly higher density in the ventral zone (-2 ± 135 HU) amongst all other groups in *post hoc* comparisons (all BKY $P < 0.05$). Additionally, both Group 3 and Group 4 showed significantly higher lung density in the dorsal zone compared to other groups in *post hoc* comparisons (30 ± 125 and 150 ± 59 HU, respectively, all adjusted $P < 0.05$).

Representative histological sections (Fig. 9*C* and *D*), obtained from the same animals shown in the CT scans, confirm these findings, revealing an increased mean alveolar tissue percentage, assessed via stereological techniques. The mean alveolar tissue percentage increased with rising DP levels and decreasing RR, with Groups 4 exhibiting significantly higher values amongst all groups in *post hoc* comparisons ($61 \pm 11\%$, respectively, all BKY $P < 0.05$; Fig. 9*F*).

A strong positive correlation was found between hypoaerated lung volume and alveolar tissue percentage ($r = 0.47$, $P = 0.0314$, Fig. 9*G*), and between DP_L and alveolar tissue percentage ($r = 0.44$, $P = 0.0.188$ Fig. 9*H*).

© 2025 The Author(s). *The Journal of Physiology* published by John Wiley & Sons Ltd on behalf of The Physiological Society.

14697793, 2026, 3, Downloaded from https://physoc.onlinelibrary.wiley.com/doi/10.1113/JP289904 by Universita Milano Bicocca, Wiley Online Library on [16/03/2026]. See the Terms and Conditions (https://onlinelibrary.wiley.com/terms-and-conditions) on Wiley Online Library for rules of use; OA articles are governed by the applicable Creative Commons License

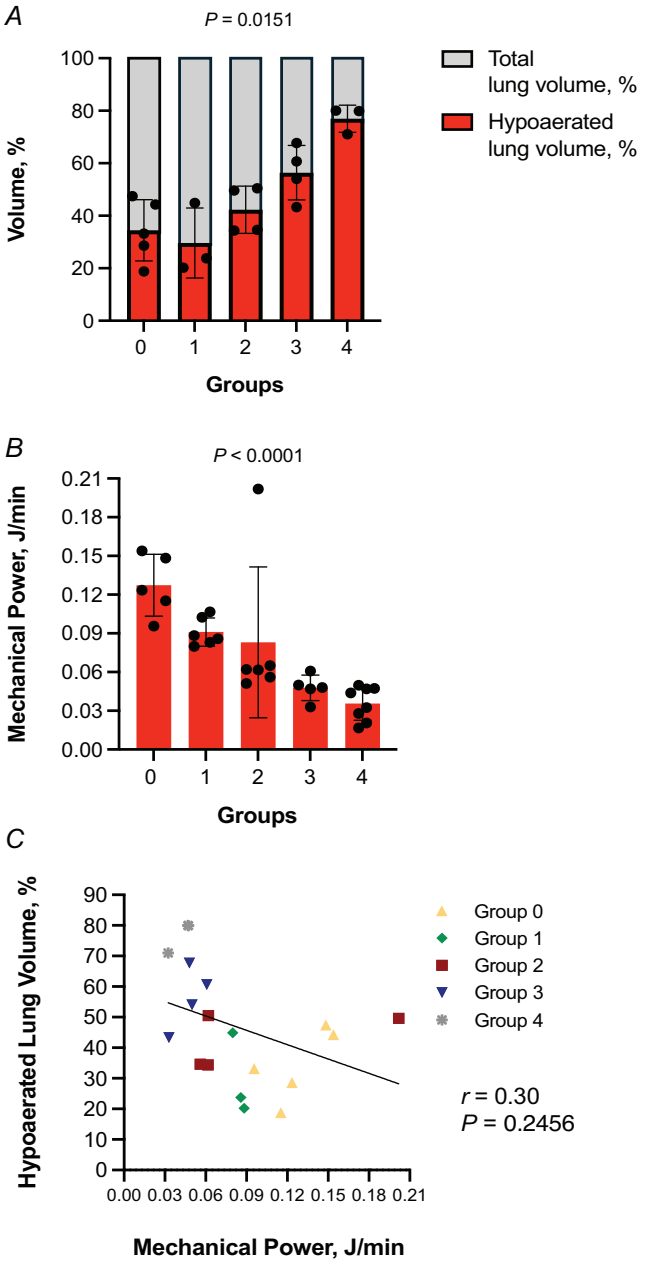

Figure 8.
Graphical representation of percentage of hypoaerated lung volume relative to total lung volume assessed by microCT (*A*), mechanical power (*B*) and correlation between mechanical power and hypoaerated lung volume in individual animals (*C*). Bars represent the mean, error bars represent SD, and each dot represents an individual animal. *P*-values (*A* and *B*) correspond to ordinary one-way ANOVA or Kruskal–Wallis test. Pearson correlation coefficient (*r*) with corresponding *P*-value is shown in panel *C*. *n* = 3–8 animals per group. MP, mechanical power.

Discussion

In this study, it was demonstrated that increasing DP levels and decreasing RR within the same 4DP+RR value is more injurious to the lungs than decreasing DP levels and increasing RR, in both healthy and lung-injured rats.

The main findings of this preclinical investigation can be summarised as follows:

(1) Keeping 4DP+RR constant whilst modifying DP and RR does not result in uniform lung injury – higher DP combined with lower RR leads to greater damage compared to maintaining a lower DP and increasing RR.
(2) The impact of increasing DP whilst decreasing RR is more pronounced in pre-injured lungs, whereas in healthy lungs this effect appears reduced.
(3) The higher severity of injury observed by increasing DP and reducing RR within the same 4DP+RR, as highlighted by the microCT scan of the lung and histological analysis, robustly correlates with the transpulmonary driving pressure.
(4) Variations in DP and RR lead to changes in MP, which is inversely associated with lung injury, as observed at the microCT scan of the lungs. This suggests that the weight of DP and RR in MP estimation may not fully reflect their contributions to VILI.

In Series 1, the observations indicate that pathophysiological indicators – including gas exchange impairment, changes in C_{rs}, W/D ratio, microCT findings, histological alterations and microscopic markers including BAL protein levels and PMNs expression – exhibit a parallel progression, becoming evident at particularly high DP levels and low RR. However, the early rise in BAL PMNs compared to protein leakage and structural changes indicates that inflammatory activation precedes overt alveolar–capillary barrier disruption. This supports the hypothesis that inflammation is an early event in VILI pathogenesis and may serve as a trigger for subsequent epithelial and endothelial injury (Slutsky & Ranieri 2013). The W/D ratio further supports this interpretation, indicating a progressive increase in extravascular lung water, consistent with barrier compromise and interstitial oedema at higher DP levels (Hales et al., 2001).

In contrast, in Series 2, there is a linear progression of damage across both pathophysiological and microscopic aspects. All evaluated parameters suggest worsening damage as DP increases and RR decreases, potentially reflecting early barrier disruption induced by hydrochloric acid. However, PMNs show a significant increase already at DP = 20 cmH_2O, possibly attributed to the use of DP levels exceeding the 'safe' threshold of 15 cmH_2O demonstrated by Amato et al. (2015).

© 2025 The Author(s). *The Journal of Physiology* published by John Wiley & Sons Ltd on behalf of The Physiological Society.

14697793, 2026, 3, Downloaded from https://physoc.onlinelibrary.wiley.com/doi/10.1113/JP289904 by Universita Milano Bicocca, Wiley Online Library on [16/03/2026]. See the Terms and Conditions (https://onlinelibrary.wiley.com/terms-and-conditions) on Wiley Online Library for rules of use; OA articles are governed by the applicable Creative Commons License

Histological assessment confirmed that structural damage increased in severity with rising DP, characterised by alveolar septal thickening, inflammatory infiltrates and haemorrhage in the most extreme groups. These alterations were paralleled by a progressive reduction in C_{rs} and impaired oxygenation, supporting a strong association between mechanical deformation and tissue-level injury (Dreyfuss et al., 1985). This relationship was particularly pronounced in Series 2, where histology revealed more widespread and severe injury patterns even at intermediate DP levels, likely due to the pre-existing epithelial injury induced by hydrochloric acid. Inter-

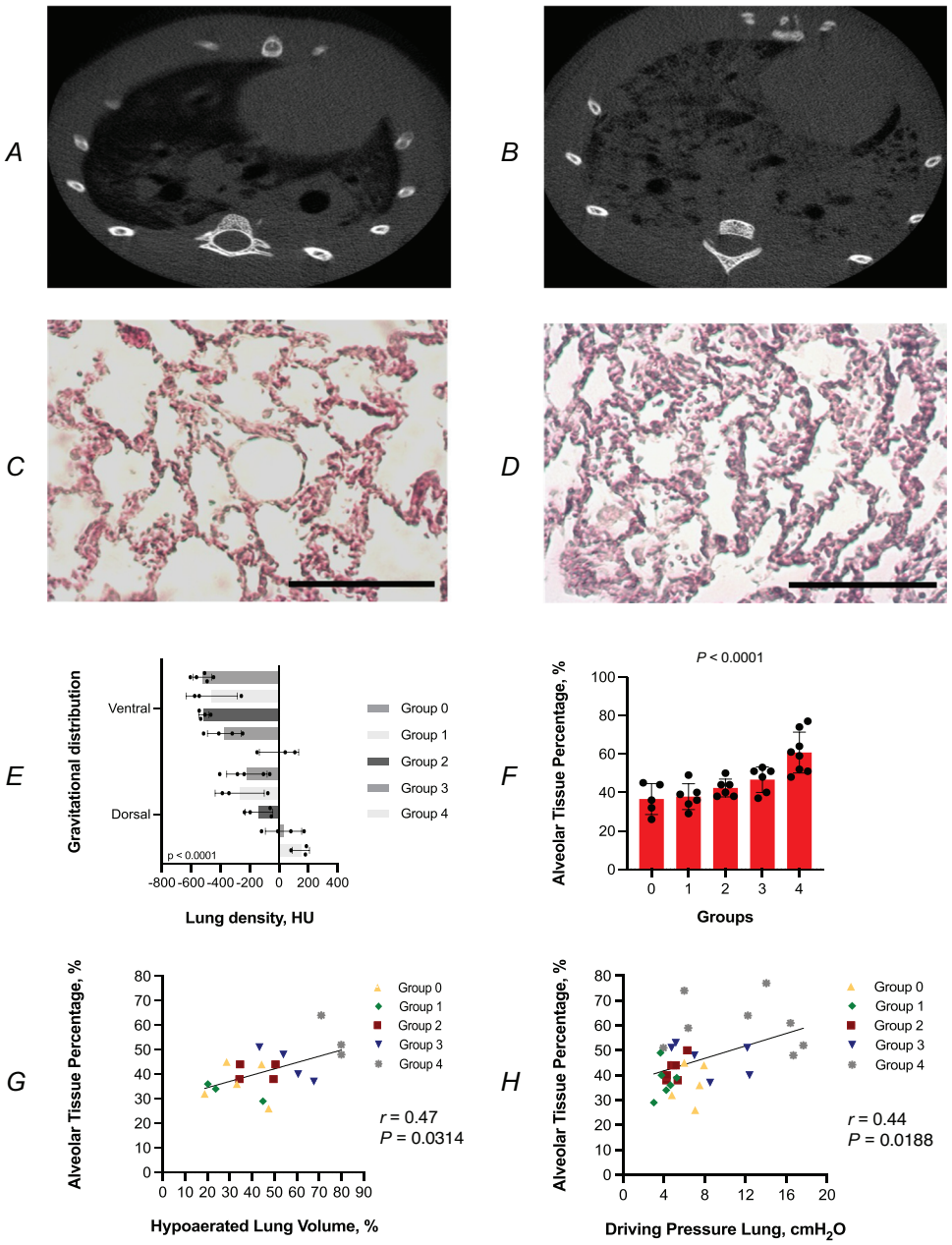

Figure 9.
Representative CT images for Group 0 (*A*) and Group 4 (*B*); representative histological sections from the same animals for Group 0 (*C*) and Group 4 (*D*); lung density variations across different gravitational levels in ventral and dorsal lung areas across groups (*E*); mean alveolar tissue percentage (*F*); correlation between hypoaerated lung volume and alveolar tissue percentage (*G*); correlation between DP_L and alveolar tissue percentage (*H*). For lung histology images, scale bar = 100 µm. Bars represent the mean, error bars represent SD, and each dot represents an individual animal. *P*-values (*E*-*F*) correspond to ordinary one-way ANOVA or Kruskal–Wallis test. Pearson correlation coefficients (*r*) with corresponding *P*-values are reported in panels *G* and *H*. *n* = 3–8 animals per group.

© 2025 The Author(s). *The Journal of Physiology* published by John Wiley & Sons Ltd on behalf of The Physiological Society.

14697793, 2026, 3, Downloaded from https://physoc.onlinelibrary.wiley.com/doi/10.1113/JP289904 by Universita Milano Biococa, Wiley Online Library on [16/03/2026]. See the Terms and Conditions (https://onlinelibrary.wiley.com/terms-and-conditions) on Wiley Online Library for rules of use; OA articles are governed by the applicable Creative Commons License

estingly, in Series 2, Group 0 exhibited a reduction in C_{rs} despite regular recruitment manoeuvres performed before each measurement, possibly due to sustained low-volume ventilation leading to derecruitment or atelectasis. However, this functional impairment was not accompanied by significant alterations in microscopic injury indices.

It is important to acknowledge that the 'safe' DP threshold may vary depending on the presence of pre-existing lung injury. As observed in Series 2, the linear progression of damage suggests that injured lungs are more susceptible to VILI, even at lower DP levels. Galizia et al. (2024) demonstrated in a healthy porcine model that DP is significantly associated with lung injury, as assessed by lung weight, lung W/D ratio and histological analysis. Their findings indicate that even in previously healthy lungs, exceeding certain DP thresholds can result in measurable damage. Similarly, Cereda et al. (2016) demonstrated through CT-based visualisation that thresholds of strain – defined as the lung deformation induced by the volume and evaluated as the ratio of volume of gas inflated to the functional residual capacity (Rezoagli et al., 2022) – considered safe in healthy lungs do not extrapolate to injured lungs, with pre-existing damage significantly lowering the tolerance to mechanical forces. Their findings show that even moderate ventilatory strain can worsen lung injury when the alveolar–capillary barrier is disrupted, supporting the need to adjust ventilation settings based on lung condition.

In addition, recent evidence suggests that it is not only the total amount of delivered energy but also its spatial and temporal distribution that determines the extent of injury, with a particular concentration in regions undergoing dynamic alveolar recruitment and derecruitment leading to greater damage (Gaver et al., 2025). Interestingly, in our experiment, the most pronounced deterioration in lung function occurred between Groups 3 and 4 for both series, where not only was DP higher, but RR markedly decreased – effectively altering the timing of respiratory cycles (prolonged expiratory phase and lower mean intrathoracic pressure) – suggesting that both variables act synergistically to exacerbate lung stress and strain. The combination of overdistension and cyclic recruitment/derecruitment is described as maximising local energy dissipation, resulting in structural injury, especially in pre-injured lungs where barrier dysfunction and surfactant deactivation amplify regional stress concentration (Fujioka et al., 2025; Gaver et al., 2020).

To compare healthy and injured animals, the findings suggest a marked reduction in lung functional reserve in Series 2. This reduction, driven by the combined effect of acid injury and ventilation, was not seen in Series 1. The double hit appears to limit the lung's ability to tolerate strain, affecting how it responds to ventilation. Recognising this is important for interpreting the outcomes. The interaction between prior injury and mechanical ventilation may have synergistic or compounding effects, exacerbating lung dysfunction. This concept aligns with findings from Buiteman-Kruizinga et al. (2025), who identified peak pressure and RR as critical determinants of MP in patients without ARDS. This study suggests that even in healthy individuals, modifying these parameters can influence the risk of VILI. Specifically, reducing RR whilst compensating with increased V_T may partially mitigate MP. This observation is consistent with the experiments by Protti et al. (2011) and Cressoni et al. (2016), which emphasise the pivotal role of RR in determining whether a given strain becomes injurious. The study by El-Khatib et al. (2024) provides further insight into the role of intraoperative MP as a key determinant of postoperative pulmonary complications, even in low-risk surgical patients.

MicroCT imaging provided significant mechanistic insight into regional lung aeration at the end of the experiment, under standardised volume-controlled ventilation ($V_T = 6$ mL/kg). This setting allowed comparison across groups. Although microCT does not provide direct measurements of regional compliance, ventilation distribution or tissue stress, the observed correlation between hypoaerated lung volume and DP_L suggests that reductions in functional lung size may be associated with impaired mechanical behaviour. These findings support the concept that lung aeration patterns can influence the mechanical vulnerability of the lung, particularly in the presence of pre-existing injury (Gattinoni et al., 2016).

In both series of rats, the contribution of the DP_{cw} to the calculation of the DP_{rs} was found to be minimal, offering little apparent protection against overdistension in groups exposed to high DP and low RR. The systematic evaluation of the combined contributions of the lungs and chest wall to respiratory mechanics is notably absent in commonly used small animals within respiratory research (Südy et al., 2019). These data underscore the feasibility of evaluating partitioned mechanics parameters through respiratory system mechanical measurements.

Finally, in this experiment, MP does not accurately reflect the extent of VILI in both series of animals. The group with the greatest damage (Group 4) exhibits the lowest value of MP. As recently discussed by da Silva et al. (2025), mechanical power alone is insufficient to account for VILI; rather, the way its components are applied – such as the relative contribution of DP and RR – plays a crucial role in determining damage from a given power value. This concept aligns with our findings, where lower MP associated with high DP and low RR still resulted in significant injury.

These mechanistic findings about the limited role of MP in characterising the lung injury play a pivotal role even

© 2025 The Author(s). *The Journal of Physiology* published by John Wiley & Sons Ltd on behalf of The Physiological Society.

14697793, 2026, 3, Downloaded from https://physoc.onlinelibrary.wiley.com/doi/10.1113/JP289904 by Universita Milano Bicocca, Wiley Online Library on [16/03/2026]. See the Terms and Conditions (https://onlinelibrary.wiley.com/terms-and-conditions) on Wiley Online Library for rules of use; OA articles are governed by the applicable Creative Commons License

in interpreting the recent clinical findings that describe a poor outcome prognostication of MP in patients with ARDS (Rezoagli et al., 2025).

An indispensable consideration for the clinical applicability of MP involves its normalisation to lung size. This normalisation is important because the energy needed to ventilate a rat or a human differs, which influences safety limits. The safe threshold for MP evaluated in an experimental investigation with 30 kg pigs show an upper limit of 12 J/min and a lower range of 4–7 J/min (Romitti et al., 2022), whilst the range observed in this study was significantly lower. These findings reinforce the complexities involved in normalising MP across different species and physiological conditions, and highlight the necessity for further research to establish precise normalisation methods (Vasques et al., 2018).

This work highlights the intricate relationship between ventilatory parameters and lung damage, highlighting the importance of optimising DP and RR in mechanical ventilation strategies. The observed early inflammatory response in Series 1 suggests that cytological changes may anticipate macroscopic evidence of lung damage, emphasising the need for vigilant monitoring and adjustments in ventilator settings to prevent or mitigate lung injury. In Series 2, the linear progression of damage across various parameters reinforces the detrimental impact of high DP and low RR.

Additional research could further enhance the understanding of the inflammatory response and provide comprehensive insights into the mechanisms underlying VILI in both healthy and damaged lung conditions.

Limitations

This study has several limitations. First, it was conducted in a rat model and caution should be applied when generalising these findings in a clinical scenario. Second, the value of 4DP+RR = 140 chosen for the experiment is different from the human physiological value, based on rat respiratory physiology (V_T and RR) (Schwarte et al., 2000). Third, an F_{IO_2} of 1 was used for all groups to prevent early death in lung-damaged groups with higher DP and lower RR. Although the risk of reabsorption atelectasis was mitigated by performing a recruitment manoeuvre every hour before the C_{rs} evaluation, this may not be completely excluded. Fourth, the experimental duration was limited to 4 h in Series 1 and 2 h in Series 2 to avoid premature animal euthanasia. Fifth, the effect of long-term application of the set ventilation procedures deserves further assessment. Sixth, severe hyperventilation may have occurred in groups with low DP and high RR, because of maintaining a constant 4DP+RR value. Although this reflects the theoretical behaviour of the index under experimental conditions, the potential confounding effects of respiratory alkalosis or hypocapnia on lung injury cannot be excluded. Finally, the extreme combination of very low RR and very high DP used in some experimental groups may limit direct clinical applicability. In ARDS patients with high ventilatory demands, maintaining adequate minute ventilation and safe pH/CO_2 levels typically requires higher RR, unless extracorporeal support is available. Therefore, whilst our findings provide mechanistic insights into VILI, caution should be used when translating these results to the clinical setting.

References

Akoumianaki, E., Maggiore, S. M., Valenza, F., Bellani, G., Jubran, A., Loring, S. H., Pelosi, P., Talmor, D., Grasso, S., Chiumello, D., Gué Rin, C., Patroniti, N., Ranieri, V. M., Gattinoni, L., Nava, S., Terragni, P. P., Pesenti, A., Tobin, M., Mancebo, J., & Brochard, L. (2014). The application of esophageal pressure measurement in patients with respiratory failure. *American Journal of Respiratory and Critical Care Medicine*, **189**(5), 520–531.

Amato, M. B. P., Meade, M. O., Slutsky, A. S., Brochard, L., Costa, E. L. V., Schoenfeld, D. A., Stewart, T. E., Briel, M., Talmor, D., Mercat, A., Richard, J.-C. M., Carvalho, C. R. R., & Brower, R. G. (2015). Driving pressure and survival in the acute respiratory distress syndrome. *New England Journal of Medicine*, **372**(8), 747–755.

Baydur, A., Behrakis, P. K., Zin, W. A., Jaeger, M., & Milic-Emili, J. (1982). A simple method for assessing the validity of the esophageal balloon technique. *The American Review of Respiratory Disease*, **126**(5), 788–791.

Bellani, G., Guerra, L., Musch, G., Zanella, A., Patroniti, N., Mauri, T., Messa, C., & Pesenti, A. (2011). Lung regional metabolic activity and gas volume changes induced by tidal ventilation in patients with acute lung injury. *American Journal of Respiratory and Critical Care Medicine*, **183**(9), 1193–1199.

Buiteman-Kruizinga, L. A., Meenen, D. M. P., Neto, A. S., Mazzinari, G., Bos, L. D. J., van der Heiden, P. L. J., Paulus, F., Schultz, M. J., & NEBULAE; PReVENT; RELAx; investigators. (2025). Association of ventilation volumes, pressures and rates with the mechanical power of ventilation in patients without acute respiratory distress syndrome: Exploring the impact of rate reduction. *Anaesthesia*, **80**(5), 533–542.

Cereda, M., Xin, Y.i, Meeder, N., Zeng, J., Jiang, Y., Hamedani, H., Profka, H., Kadlecek, S., Clapp, J., Deshpande, C. G., Wu, J., Gee, J. C., Kavanagh, B. P., & Rizi, R. R. (2016). Visualizing the propagation of acute lung injury. *Anesthesiology*, **124**(1), 121–131.

Chiumello, D., Gotti, M., Guanziroli, M., Formenti, P., Umbrello, M., Pasticci, I., Mistraletti, G., & Busana, M. (2020). Bedside calculation of mechanical power during volume- and pressure-controlled mechanical ventilation. *Critical Care*, **24**(1), 1–8.

© 2025 The Author(s). *The Journal of Physiology* published by John Wiley & Sons Ltd on behalf of The Physiological Society.

14697793, 2026, 3, Downloaded from https://physoc.onlinelibrary.wiley.com/doi/10.1113/JP289904 by Universita Milano Bicocca, Wiley Online Library on [16/03/2026]. See the Terms and Conditions (https://onlinelibrary.wiley.com/terms-and-conditions) on Wiley Online Library for rules of use; OA articles are governed by the applicable Creative Commons License

Costa, E. L. V., Slutsky, A. S., Brochard, L. J., Brower, R., Serpa-Neto, A., Cavalcanti, A. B., Mercat, A., Meade, M., Morais, C. C. A., Goligher, E., Carvalho, C. R. R., & Amato, M. B. P. (2021). Ventilatory variables and mechanical power in patients with acute respiratory distress syndrome. *American Journal of Respiratory and Critical Care Medicine*, **204**(3), 303–311.

Cressoni, M., Gotti, M., Chiurazzi, C., Massari, D., Algieri, I., Amini, M., Cammaroto, A., Brioni, M., Montaruli, C., Nikolla, K., Guanziroli, M., Dondossola, D., Gatti, S., Valerio, V., Vergani, G. L., Pugni, P., Cadringher, P., Gagliano, N., & Gattinoni, L. (2016). Mechanical power and development of ventilator-induced lung injury. *Anesthesiology*, **124**(5), 1100–1108.

da Silva, A. L., Magalhaes, R. F., Conceicao, P. H. L., Santos, A. C. M. D., Oliveira, C. M., Thorton, L. T., Crooke, P. S., Baldavira, C. M., Capelozzi, V. L., Cruz, F. F., Samary, C. S., Silva, P. L., Marini, J. J., & Rocco, P. R. M. E. (2025). Effects of similar mechanical power resulting from different combinations of respiratory variables on lung damage in experimental acute Respiratory distress syndrome. *Critical Care Medicine*, **53**(6), e1303–e1313.

Dassow, C., Schwenninger, D., Runck, H., & Guttmann, J. (2013). Time and volume dependence of dead space in healthy and surfactantdepleted rat lungs during spontaneous breathing and mechanical ventilation. *Journal of Applied Physiology*, **115**(9), 1268–1274.

Díaz, L., Zambrano, E., Flores, M. E., Contreras, M., Crispín, J. C., Alemán, G., Bravo, C., Armenta, A., Valdés, V. J., Tovar, A., Gamba, G., Barrios-Payán, J., & Bobadilla, N. A. (2020). Ethical considerations in animal research: The principle of 3R's. *Revista de Investigacion Clinica; Organo Del Hospital de Enfermedades de La Nutricion*, **73**(4), 199–209.

Docci, M., Beloncle, F., Lesimple, A., Piraino, T., Cominesi, D. R., Restivo, A., Mayson, L. A. Sousa, E. Rezoagli, A. Mercat, J. Richard, C., Brochard, L., & CAVIAR Group. (2025). Erroneous calibration of esophageal pressure in case of airway closure. *Critical Care*, **29**(1), 178.

Dreyfuss, D., Basset, G., Soler, P., & Saumon, G. (1985). Intermittent positive-pressure hyperventilation with high inflation pressures produces pulmonary microvascular injury in rats. *The American Review of Respiratory Disease*, **132**(4), 880–884.

Dreyfuss, D., & Hubmayr, R. (2016). What the concept of VILI has taught us about ARDS management. *Intensive Care Medicine*, **42**(5), 811–813.

El-Khatib, M., Zeeni, C., Shebbo, F. M., Karam, C., Safi, B., Toukhtarian, A., Nafeh, N. A., Mkhayel, S., Shadid, C. A., Chalhoub, S., & Beresian, J. (2024). Intraoperative mechanical power and postoperative pulmonary complications in low-risk surgical patients: A prospective observational cohort study. *BioMed Central Anesthesiology*, **24**(1), 1–9.

Fujioka, H., Halpern, D., & Gaver, D. P. 3rd (2025). Predictions of atelectasis-induced microvolutrauma: A key pathway to ventilator-induced lung injury. *Journal of Biomechanical Engineering*, **147**(10), 101003.

Fujita, Y., Fujino, Y., Uchiyama, A., Mashimo, T., & Nishimura, M. (2007). High peak inspiratory flow can aggravate ventilator-induced lung injury in rabbits. *Medical Science Monitor : International Medical Journal of Experimental and Clinical Research*, **13**(4), BR95–BR100.

Gajic, O., Frutos-Vivar, F., Esteban, A., Hubmayr, R. D., & Anzueto, A. (2005). Ventilator settings as a risk factor for acute Respiratory distress syndrome in mechanically ventilated patients. *Intensive Care Medicine*, **31**(7), 922–926.

Galizia, M., Ghidoni, V., Catozzi, G., Giovanazzi, S., Nocera, D., Donati, B., Pozzi, T., D'Albo, R., Busana, M., Romitti, F., Herrmann, P., Moerer, O., Meissner, K., Quintel, M., Camporota, L., & Gattinoni, L. (2024). Predictors of VILI risk: Driving pressure, 4DPRR and mechanical power ratio—An experimental study. *Intensive Care Medicine Experimental*, **12**(1), 116.

Gattinoni, L., Tonetti, T., Cressoni, M., Cadringher, P., Herrmann, P., Moerer, O., Protti, A., Gotti, M., Chiurazzi, C., Carlesso, E., Chiumello, D., & Quintel, M. (2016). "Ventilator-related causes of lung injury: The mechanical power." *Intensive Care Medicine*, **42**(10), 1567–1575.

Gattinoni, L., Marini, J. J., Pesenti, A., Quintel, M., Mancebo, J., & Brochard, L. (2016). The 'baby lung' became an adult. *Intensive Care Medicine*, **42**(5), 663–673.

Gaver, D. P. 3rd, Kollisch-Singule, M., Nieman, G., Satalin, J., Habashi, N., & Bates, J. H. T. (2025). Mechanical ventilation energy analysis: Recruitment focuses injurious power in the ventilated lung. *Proceedings of the National Academy of Sciences of the United States of America*, **122**(10), e2419374122.

Gaver, D. P., Nieman, G. F., Gatto, L. A., Cereda, M., Habashi, N. M., & Bates, J. H. T. (2020). The POOR get POORer: A hypothesis for the pathogenesis of ventilator-induced lung injury. *American Journal of Respiratory and Critical Care Medicine*, **202**(8), 1081–1087.

Hales, C. A., Du, H. K., Volokhov, A., Mourfarrej, R., & Quinn, D. A. (2001). Aquaporin channels may modulate ventilator-induced lung injury. *Respiration Physiology*, **124**(2), 159–166.

Hopkins, N., Cadogan, E., Giles, S., & McLoughlin, P. (2001). Chronic airway infection leads to angiogenesis in the pulmonary circulation. *Journal of Applied Physiology*, **91**(2), 919–928.

Horie, S., Gonzalez, H., Brady, J., Devaney, J., Scully, M., O'toole, D., & Laffey, J. G. (2021). Fresh and cryopreserved human umbilical-cord-derived mesenchymal stromal cells attenuate injury and enhance resolution and repair following ventilation-induced lung injury. *International Journal of Molecular Sciences*, **22**(23), 12842.

Lee, W. L., & Slutsky, A. S. (2001). Ventilator-induced lung injury and recommendations for mechanical ventilation of patients with ARDS. *Seminars in Respiratory and Critical Care Medicine*, **22**(3), 269–280.

Magliocca, A., Rezoagli, E., Zani, D., Manfredi, M., de Giorgio, D., Olivari, D., Fumagalli, F., Langer, T., Avalli, L., Grasselli, G., Latini, R., Pesenti, A., Bellani, G., & Ristagno, G. (2021). Cardiopulmonary resuscitation–Associated lung edema (CRALE): A translational study. *American Journal of Respiratory and Critical Care Medicine*, **203**(4), 447–457.

© 2025 The Author(s). *The Journal of Physiology* published by John Wiley & Sons Ltd on behalf of The Physiological Society.

14697793, 2026, 3, Downloaded from https://physoc.onlinelibrary.wiley.com/doi/10.1113/JP289904 by Universita Milano Bicocca, Wiley Online Library on [16/03/2026]. See the Terms and Conditions (https://onlinelibrary.wiley.com/terms-and-conditions) on Wiley Online Library for rules of use; OA articles are governed by the applicable Creative Commons License

Magliocca, A., Zani, D., Zani, D. D.e, Castagna, V., Merigo, G., Giorgio, D. D., Fumagalli, F., Zambelli, V., Boccardo, A., Pravettoni, D., Bellani, G., Richard, J. C., Grasselli, G., Rezoagli, E., & Ristagno, G. (2024). A multimodal characterization of cardiopulmonary resuscitation-associated lung edema. *Intensive Care Medicine Experimental*, **12**(1), 91.

Moraes, L., Silva, P. L., Thompson, A., Santos, C. L., Santos, R. S., Fernandes, M. V. S., Morales, M. M., Martins, V., Capelozzi, V. L., de Abreu, M. G., Pelosi, P., & Rocco, P. R. M. (2018). Impact of different tidal volume levels at low mechanical power on ventilator-induced lung injury in rats. *Frontiers in Physiology*, **9**(APR), 1–12.

Pecchiari, M., Monaco, A., Koutsoukou, A., Valle, P. D., Gentile, G., & D'Angelo, E. (2014). Effects of various modes of mechanical ventilation in normal rats. *Anesthesiology*, **120**(4), 943–950.

Protti, A., Cressoni, M., Santini, A., Langer, T., Mietto, C., Febres, D., Chierichetti, M., Coppola, S., Conte, G., Gatti, S., Leopardi, O., Masson, S., Lombardi, L., Lazzerini, M., Rampoldi, E., Cadringher, P., & Gattinoni, L. (2011). Lung stress and strain during mechanical ventilation: Any safe threshold?. *American Journal of Respiratory and Critical Care Medicine*, **183**(10), 1354–1362.

Reiss, L. K., Kowallik, A., & Uhlig, S. (2011). Recurrent recruitment manoeuvres improve lung mechanics and minimize lung injury during mechanical ventilation of healthy mice. *PLoS ONE*, **6**(9), e24527.

Rezoagli, E., Laffey, J. G., & Bellani, G. (2022). Monitoring lung injury severity and ventilation intensity during mechanical ventilation. *Seminars in Respiratory and Critical Care Medicine*, **43**(3), 346–368.

Rezoagli, E., Laffey, J. G., Madotto, F., Protti, A., Pham, T., Pesenti, A., Bellani, G., Brochard, L., & LUNG SAFE Investigators and the ESICM Trials Group. (2025). Prognostic value of disease severity and mechanical ventilation intensity in Acute Respiratory Distress Syndrome. Analysis of the LUNG SAFE cohort. *The European Respiratory Journal*, **67**(1), 2500742.

Rezoagli, E., Magliocca, A., Luca Grieco, D., Bellani, G., & Ristagno, G. (2022). Impact of lung structure on airway opening index during mechanical versus manual chest compressions in a porcine model of cardiac arrest. *Respiratory Physiology & Neurobiology*, **296**, 103807.

Rich, P. B., Douillet, C. D., Hurd, H., & Boucher, R. C. (2003). Effect of ventilatory rate on airway cytokine levels and lung injury. *The Journal of Surgical Research*, **113**(1), 139–145.

Romitti, F., Busana, M., Palumbo, M. M., Bonifazi, M., Giosa, L., Vassalli, F., Gatta, A., Collino, F., Steinberg, I., Gattarello, S., Lazzari, S., Palermo, P., Nasr, A., Kathrin Gersmann, A., Richter, A., Herrmann, P., Moerer, O., Saager, L., Camporota, L., … Gattinoni, L. (2022). Mechanical power thresholds during mechanical ventilation: An experimental study. *Physiological Reports*, **10**(6), 1–10.

Schwarte, L. A., Zuurbier, C. J., & Ince, C. (2000). Mechanical ventilation of mice. *Basic Research in Cardiology*, **95**(6), 510–520.

Slutsky, A. S., & Ranieri, V. M. (2013). Ventilator-induced lung injury. *The New England Journal of Medicine*, **369**(22), 2126–2136.

Südy, R., Fodor, G. H., Rocha, A. D. S., Schranc, Á.l., Tolnai, J., Habre, W., & Peták, F. (2019). Different contributions from lungs and chest wall to Respiratory mechanics in mice, rats, and rabbits. *Journal of Applied Physiology*, **127**(1), 198–204.

Tonetti, T., Vasques, F., Rapetti, F., Maiolo, G., Collino, F., Romitti, F., Camporota, L., Cressoni, M., Cadringher, P., Quintel, M., & Gattinoni, L. (2017). Driving pressure and mechanical power: New targets for VILI prevention. *Annals of Translational Medicine*, **5**(14), 1–10.

Tremblay, L. N., & Slutsky, A. S. (1998). Ventilator-induced injury: From Barotrauma to Biotrauma. *Proceedings of the Association of American Physicians*, **110**(6), 482–488.

Vasques, F., Duscio, E., Pasticci, I., Romitti, F., Vassalli, F., Quintel, M., & Gattinoni, L. (2018). Is the mechanical power the final word on ventilator-induced lung injury?—We are not sure. *Annals of Translational Medicine*, **6**(19), 395–395.

Zambelli, V., Murphy, E. J., Delvecchio, P., Rizzi, L., Fumagalli, R., Rezoagli, E., & Bellani, G. (2023). Treatment with Levosimendan in an experimental model of early ventilator-induced diaphragmatic dysfunction. *Drug Target Insights*, **17**(8), 39–44.

Additional information

Data availability statement

All data supporting the findings of this study are included within the manuscript figures and tables. Additional information is available from the corresponding author upon reasonable request.

Competing interests

The authors declare they have no conflicts of interest.

Author contributions

D.R.C., V.Z., R.G., A.M., and E.R. performed experiments. D.R.C., V.Z., and E.R. analysed data. D.R.C., V.Z., and E.R. drafted the manuscript. D.R.C., V.Z., E.J.M., R. G., A.M., G.F., M.C., J.G.L., and E.R. edited the manuscript. D.R.C., V.Z., E.J.M., R.G., A.M., R.F., G.B., G.F., M.C., J.G.L., and E.R. revised the manuscript. D.R.C., V.Z., E.J.M., R.G., A.M., G.F., M.C., J.G.L., and E.R. interpreted the results of experiments. D.R.C., V.Z., E.J.M., and E.R. prepared figures. E.R. conceived and designed the research, supervised the overall project and is the guarantor of the overall study project. All authors have approved the final version of the manuscript and agree to be accountable for all aspects of the work in ensuring that questions related to the accuracy or integrity of any part of the work are appropriately investigated and resolved. All persons designated as authors qualify for authorship, and all those who qualify for authorship are listed.

© 2025 The Author(s). *The Journal of Physiology* published by John Wiley & Sons Ltd on behalf of The Physiological Society.

14697793, 2026, 3, Downloaded from https://physoc.onlinelibrary.wiley.com/doi/10.1113/JP289904 by Universita Milano Bicocca, Wiley Online Library on [16/03/2026]. See the Terms and Conditions (https://onlinelibrary.wiley.com/terms-and-conditions) on Wiley Online Library for rules of use; OA articles are governed by the applicable Creative Commons License

Funding

The study was supported by internal research funding of Prof. Emanuele Rezoagli at the University of Milano-Bicocca, Monza, Italy. No external funding was received for this work.

Keywords

acute lung injury, driving pressure, mechanical ventilation, respiratory rate, ventilator-induced lung injury

Supporting information

Additional supporting information can be found online in the Supporting Information section at the end of the HTML view of the article. Supporting information files available:

Peer Review History

© 2025 The Author(s). *The Journal of Physiology* published by John Wiley & Sons Ltd on behalf of The Physiological Society.

14697793, 2026, 3, Downloaded from https://physoc.onlinelibrary.wiley.com/doi/10.1113/JP289904 by Universita Milano Bicocca, Wiley Online Library on [16/03/2026]. See the Terms and Conditions (https://onlinelibrary.wiley.com/terms-and-conditions) on Wiley Online Library for rules of use; OA articles are governed by the applicable Creative Commons License